RZ 3937 (# ZUR1802-063) 02/23/2018
Physical Sciences 39 pages

# Research Report

## Atomic force microscopy identifying fuel pyrolysis products and directing the synthesis of analytical standards

Shadi Fatayer[1], Nimesh B. Poddar[2], Sabela Quiroga[3], Fabian Schulz[1], Bruno Schuler[1Ψ], Subramanian V. Kalpathy[2], Gerhard Meyer[1], Dolores Pérez[3], Enrique Guitián[3], Diego Peña[3], Mary J. Wornat[2], Leo Gross[1]

[1] IBM Research-Zurich, Rüschlikon 8803, Switzerland
[2] Department of Chemical Engineering, Louisiana State University, Baton Rouge, Louisiana 70803, United States
[3] Centro Singular de Investigación en Química Biolóxica e Materiais Moleculares (CiQUS), Departamento de Química Orgánica, Universidade de Santiago de Compostela. Santiago de Compostela 15782, Spain
[Ψ] Current address: Molecular Foundry, Lawrence Berkeley National Laboratory, California 94720, USA

**Atomic force microscopy identifying fuel pyrolysis products and directing the synthesis of analytical standards**

Shadi Fatayer,[1] Nimesh B. Poddar,[2] Sabela Quiroga,[3] Fabian Schulz,[1] Bruno Schuler,[1Ψ] Subramanian V. Kalpathy,[2] Gerhard Meyer,[1] Dolores Pérez,[3] Enrique Guitián,[3] Diego Peña,[3*] Mary J. Wornat,[2*] Leo Gross[1*]

*1. IBM Research–Zurich, 8803 Rüschlikon, Switzerland*

*2. Department of Chemical Engineering, Louisiana State University, Baton Rouge, Louisiana 70803, United States*

*3. Centro Singular de Investigación en Química Biolóxica e Materiais Moleculares (CiQUS), Departamento de Química Orgánica, Universidade de Santiago de Compostela. Santiago de Compostela 15782, Spain*

**diego.pena@usc.es, *mjwornat@lsu.edu, *lgr@zurich.ibm.com*

[Ψ] Current address: Molecular Foundry, Lawrence Berkeley National Laboratory, California 94720, USA

**Abstract**

Here we present a new method that integrates atomic force microscopy (AFM) with analytical tools such as high-performance liquid chromatography (HPLC) with diode-array ultraviolet-visible (UV) absorbance and mass spectrometry (MS) along with synthetic chemistry. This allows the detection, identification, and quantification of novel polycyclic aromatic hydrocarbons (PAH) in complex molecular mixtures. This multi-disciplinary methodology is employed to characterize the supercritical pyrolysis products of *n*-decane, a model fuel. The pyrolysis experiments result in a complex mixture of both unsubstituted as well as highly methylated PAH. We demonstrate the AFM-driven discovery of a novel compound, benz[*l*]indeno[1,2,3-*cd*]pyrene, with the chemical structure assignment serving as input for the chemical synthesis of such molecule. The synthesis is verified by AFM and the synthesized compound is used as a reference standard in analytical measurements, establishing the first-ever unequivocal identification and quantification of this PAH as a fuel product. Moreover, the high-resolution AFM analysis detected several five- to eight-ring PAH, which represents novel fuel pyrolysis and/or combustion products. This work provides a route to develop new analytical standards by symbiotically using AFM, chemical synthesis, and modern analytical tools.

Keywords: atomic force microscopy; CO-functionalized tips; polycyclic aromatic hydrocarbons; pyrolysis; synthetic chemistry

## 1. Introduction

The investigation of complex molecular mixtures relies on the use of standards for experimental comparison.[1-7] Due to the limited number of molecular standards that are commercially available, thorough studies require the synthesis of new reference compounds. However, choosing the molecules to be synthesized for the characterization of a mixture with unknown components is challenging and often relies on the use of spectroscopic methods.[1,6,7] The synthesis of the standards itself is often expensive and time consuming. As an example, the number of possible polycyclic aromatic hydrocarbons (PAH) isomers increases significantly with increasing molecular weight.[8] Therefore, given a molecular formula, the number of unique PAH structures is large for molecules containing a combination of five- and six-membered rings. For instance, the $C_{24}H_{14}$ benzenoid PAH, with only six-membered rings, display 12 isomers. For the same molecular formula, but with two five-membered rings instead, there are a total of 266 isomers.[9] In the absence of a reference standard, other analytical methods can be employed for determining the structure of unknown PAH,[8,10] but some of these methods are limited by low concentration and need extensive purification of individual PAH in complex molecular matrices.

PAH are ubiquitous pollutants formed during the pyrolysis and/or combustion of a wide-variety of fuels and/or fuel components. The formation and subsequent growth of PAH is of practical concern for four principal reasons: (1) PAH are known precursors to soot,[11–13] which poses serious health hazards[14–16] and is a major contributor to global climate change;[17–19] (2) PAH are found in the extracts of solid deposits from catalytic hydrocracking of petroleum,[1] suggesting that PAH could be precursors to these deposits, which can clog process piping[1] and cause catalyst fouling,[20,21] resulting in process downtime; (3) Some PAH are known to be potent carcinogens and/or mutagens;[2,22–24] and (4) PAH are precursors to carbonaceous solids,[25–30] which can clog fuel lines and injection nozzles and foul heat transfer surfaces, thereby seriously jeopardizing the safe operation of future high-speed aircraft.

In the context of the pre-combustion environments[25,31] of future high-speed aircrafts, better understanding of pyrolytic reactions that lead to PAH formation and growth would facilitate the design of fuel systems that are not prone to solids formation. Therefore, we conducted supercritical pyrolysis experiments[28–30,32,33] of the model fuel *n*-decane, an *n*-alkane component of jet fuels.[34,35] An *n*-alkane fuel is chosen because, under supercritical pyrolysis conditions, these jet-fuel components exhibit a high propensity for solids formation.[25,28–30] To thoroughly understand PAH formation and growth reactions, particular emphasis is placed on the isomer-specific analysis of the PAH products by high-performance liquid chromatography (HPLC) with diode-array ultraviolet-visible (UV) absorbance and mass spectrometric (MS) detection. Previous HPLC/UV/MS analyses[28–30,32,33] of the supercritical *n*-decane pyrolysis products led to the identification of over 400 three- to nine-ring PAH, many of which contain one or more methyl functionalities. The quantification of the PAH products of supercritical *n*-decane pyrolysis reveals that the yields of higher-ring-number PAH are about an order of magnitude lower than their lower-ring-number counterparts.[28–30] In addition to the low yields of higher-ring-number PAH, *n*-decane produces many alkylated PAH, which makes the identification and quantification of PAH mixtures of $\geq$ 5 rings an enormous undertaking.

Recently, high-resolution atomic force microscopy (AFM) with CO-functionalized tips showed to be capable of identifying individual molecules[36–39] and thus, molecular mixtures can be studied molecule-by-molecule.[40–44] With this approach, details about the mechanisms of on-surface organic reactions[40,42–45] and the molecular architecture and composition of complex molecular mixtures[41,46] have been obtained. Due to the single-molecule sensitivity of AFM, the detection of molecules present in miniscule amounts is viable. Important for our study of fuel pyrolysis products, five- and six-membered carbon rings as well as various aliphatic groups can be differentiated and identified by AFM.[40,47,48].

Here we demonstrate a method that employs atomic-resolution low-temperature AFM to identify reference standards. AFM is integrated with HPLC/UV/MS and synthetic chemistry to identify

previously unidentified PAH products of fuel pyrolysis in two different steps. First, to identify unknown PAH within the PAH-product fractions of supercritical *n*-decane pyrolysis, providing candidates for the targeted synthesis of new reference standards. Second, to confirm the molecular structure of the synthesized standard. With this approach, first, a novel seven-ring PAH, benz[*l*]indeno[1,2,3-*cd*]pyrene, is identified by AFM. Subsequently, it is synthesized and then also confirmed by AFM. The synthesized standard of benz[*l*]indeno[1,2,3-*cd*]pyrene is analyzed by HPLC/UV, providing the UV absorbance spectrum, a fingerprint property of PAH, allowing the identification and quantification of this novel seven-ring PAH in an isomer-specific manner as a product of supercritical *n*-decane pyrolysis.

This method provides a powerful tool for directing the synthesis of target molecules and for the structural confirmation of synthesized molecules, thereby providing a reference standard for subsequent analysis. It is important to note that this method is not limited to a particular system but can be applied to a wide range of molecular mixtures such as those found in nature, obtained from chemical synthesis, and derived from fuel pyrolysis and/or combustion.

## 2. Experimental section

### 2.1 Pyrolysis experiments and HPLC/UV/MS analysis

The supercritical pyrolysis experiments of the model fuel *n*-decane (99.5% pure; critical temperature, 344.5 °C; critical pressure, 20.7 atm) are conducted in an isothermal, isobaric silica-lined stainless-steel flow reactor described elsewhere.[32,33] For the present study, the PAH-product mixture is obtained from supercritical *n*-decane-pyrolysis experiments performed at 570 °C, 94.6 atm, and 133 sec, respectively, conditions of high PAH production and onset of solids formation.[28–30,32,33]

The PAH products of supercritical *n*-decane pyrolysis are comprised of a complex mixture of unsubstituted PAH and their alkylated derivatives, which requires the application of a two-dimensional HPLC separation technique to achieve sufficient resolution for PAH-product identification and quantification. This HPLC separation procedure was established by Wise *et al.*[49] and further developed

by Bagley and Wornat[32,33] for the analysis of the PAH products of supercritical *n*-alkane-fuel pyrolysis. The PAH products are first fractionated by normal-phase HPLC into 15 individual fractions by isomer group and/or number of π-bonds. Therefore, an individual PAH-product fraction contains unsubstituted PAH of a particular isomer group, along with their corresponding alkylated derivatives. In the second dimension of separation, each PAH-product fraction is analyzed by reversed-phase HPLC with diode-array ultraviolet-visible (UV) absorbance and mass spectrometric (MS) detection for the isomer-specific identification of the PAH products. The quantification of these products is obtained from extensive calibration of the UV absorbance detector with PAH reference standards.

As demonstrated in our previous studies,[28-30] supercritical *n*-decane pyrolysis produces PAH products containing 2 to 10 aromatic rings, which are fraction collected based on the number of π-bonds.[32,33] For the scope of the present study, the two PAH-product fractions that are analyzed by AFM are: (1) Fraction **P**, comprised of PAH of $\geq$ 5 rings (*i.e.* of aromatic carbon number $\geq$ 20), obtained from the pre-fractionation step of our more-involved normal-phase HPLC fractionation procedure,[32,33] and (2) Fraction **F** (labelled as Fraction 11),[32,33] primarily composed of seven-ring PAH of the isomer group $C_{26}H_{14}$ (or PAH with 13 π-bonds) and their alkylated derivatives, obtained from the more-involved normal-phase HPLC fractionation procedure.[32,33]

### 2.2 AFM measurements

We performed AFM experiments by using a home-built low-temperature ($T \approx 5$ K), ultrahigh vacuum ($p \approx 1 \times 10^{-10}$ mbar) combined scanning tunneling microscopy (STM) and AFM setup. We employed a qPlus sensor[50] operated in the frequency-modulation mode[51] (resonance frequency $f_0 \approx 30$ kHz, spring constant $k \approx 1800$ N/m, quality factor $Q \approx 14{,}000$, and oscillation amplitude $A = 0.5$ Å). We applied the bias voltage $V$ to the sample. AFM measurements were acquired in constant-height mode at $V = 0$ V. As substrate we used a Cu(111) single crystal partly covered by bilayer (100)-oriented NaCl islands.[52] We deposited a low coverage (approximately 0.02 $nm^{-2}$) of CO on the surface for tip

preparation by admitting CO into the UHV chamber at a sample temperature of $T \approx 10$ K. The PAH fractions were separately prepared by spreading a small amount (on the order of 1 mg) of the solid, dry material on a piece of Si wafer. Then, the wafer was flash-heated by resistive heating in front of the cold sample.[41] For the microscope tip, we used a 25 μm-thick PtIr wire, shortened and sharpened with a focused ion beam. Thereafter, we prepared a clean and sharp Cu tip by repeated indentations into the Cu surface. Finally, a CO-functionalized tip was created by picking-up a single CO molecule from the surface.[36,53]

The assignment of the structures from the AFM images is based on previous works resolving molecules atomically by AFM with CO-functionalized tips,[36–40,42–44,48,54] taking into account the known effect of distortions due to the tilting of the CO molecule at the tip. [55,56] For example, we distinguish five- and six-membered rings by the number of bond intersections and corners and by the respective positions and enclosed angles of adjacent moieties. Methyl[41] and other aliphatic substituents[48] are assigned by their characteristic contrast that was obtained by measuring synthesized standards by AFM. The presence of substitutional heteroatoms, such as nitrogen, cannot be decisively dismissed solely based on the AFM results shown here.[37,54] However, its presence amongst the PAH products can be ruled out because there is no source of nitrogen, either in the fuel *n*-decane and/or added to the reaction system, in the supercritical *n*-decane pyrolysis experiments.

We emphasize that quantification of the abundance of compounds with the AFM is challenging, because the acquisition time is on the order of 10 min for an atomically resolved image and limits the number of molecules that can feasibly be imaged within a sample to a few hundred. A statistical analysis of AFM data and its comparison with mass spectrometry indicated the statistical significance of the sampling by AFM[46]; however, the numbers of molecules to be imaged for their quantification in complex mixtures by AFM would have to be increased by several orders of magnitude.

Because of the preparation method employed, also the maximum size of molecules that can be studied is limited. Typically, molecules of 1000 Da molecular weight or more fragment when they are sublimed[39]. The molecules investigated here are of molecular weights below 500 Da and thus fragmentation in the sublimation process is negligible. Moreover, they are mostly planar which is advantageous to obtain high resolution images with CO-tip AFM. Even considering the challenges of AFM resolving non-planar, larger and more fragile molecules, there are strategies for investigating non-planar molecules[47,57,58,59], it is also possible to investigate larger and more fragile molecules using electrospray ionization deposition[60,61,62]. We envision the methodology shown here being jointly used with these strategies. For a more detailed discussion of the pitfalls and challenges of AFM for structure elucidation we refer the reader to a recent review.[63]

## 3. Results and Discussion

By employing AFM, we first measure the supercritical *n*-decane pyrolysis product Fraction **P**. This relatively broad PAH-product fraction is analyzed by AFM to obtain an overview of the PAH produced during supercritical *n*-decane pyrolysis. AFM results showing individual PAH contained in Fraction **P** are displayed in Figure 1a. Based on the AFM measurements, a PAH structure is assigned to each AFM image. The resolved and assigned molecules in Figure 1b are: five-ring PAH **P1** and **P2**; six-ring PAH **P3**, **P4**, and **P5**; seven-ring PAH **P6** and **P7**; and eight-ring PAH **P8**. Of these eight PAH products shown in Figure 1, five are unsubstituted PAH (**P1**, **P2**, **P3**, **P6**, and **P7**) and three are methylated PAH (**P4**, **P5**, and **P8**). Additionally, these eight PAH fall under three main structural classes: benzenoid PAH (**P3**, **P4**, and **P5**), fluoranthene benzologues (**P1**, **P6**, **P7**, and **P8**), and a phenalene benzologue (**P2**). These findings are consistent with previous HPLC/UV/MS analysis of the supercritical *n*-decane pyrolysis products.[28–30,32,33]

Of the eight PAH shown in Figure 1, four (**P1**, **P3**, **P4**, and **P5**) were reported in previous HPLC/UV/MS analysis of the supercritical *n*-decane pyrolysis products.[32,33] A reference standard of **P6**

is available to us and the UV absorbance maxima of **P2** are published;[64] however, neither of these two PAH were previously identified as products of supercritical *n*-decane pyrolysis. It could be that **P2** and **P6** are present in amounts below the detection limit (0.3 ng of material) of our HPLC instrument or their chromatographic signal is being masked by one or more co-eluting higher-yield PAH products. Studies report **P6** as a pyrolysis product,[65–67] but not from fuel pyrolysis experiments. Unlike **P2** and **P6**, a reference standard and/or UV spectrum of **P8** is unavailable. Presumably, the high sensitivity of AFM due to single-molecule detection enabled us to detect **P2**, **P6**, and **P8**, which were previously not reported as fuel pyrolysis and/or combustion products.

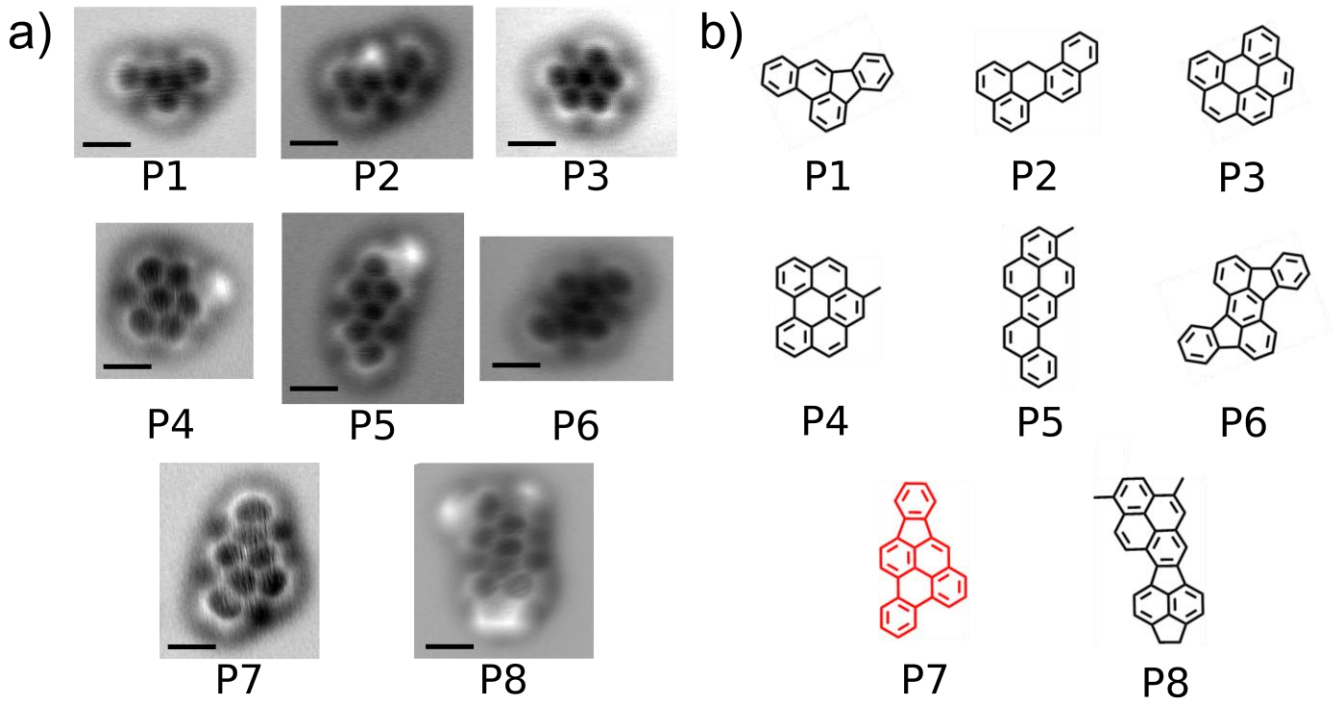


**Figure 1.** Fraction **P** of the products of *n*-decane pyrolysis at 570 °C, 94.6 atm, and 133 sec measured by AFM: (a) Constant-height AFM measurements with a CO-functionalized tip. Scale bars are 5 Å. **P1**, **P2**, **P3** and **P5** were measured on Cu(111); **P4**, **P6**, **P7**, and **P8** were measured on bilayer NaCl on Cu(111). (b) Proposed chemical structures: benzo[*b*]fluoranthene (**P1**), 7*H*-benzo[*hi*]chrysene (**P2**), benzo-[*ghi*]perylene (**P3**), 1-methylbenzo[*ghi*]perylene (**P4**), 1-methylnaphtho[2,1-*a*]pyrene (**P5**), rubicene (**P6**) benz[*l*]indeno[1,2,3-*cd*]pyrene (**P7**), and 7,10-dimethyl-1,2-dihydrocyclopenta[5,6]acenaphtho[1,2-*a*]pyrene (**P8**).

Notably, we also detected with AFM a seven-ring $C_{26}H_{14}$ PAH benz[*l*]indeno[1,2,3-*cd*]pyrene (**P7**, in Figure 1), whose synthesis and/or identification as a fuel product has previously not been reported in the literature. Therefore, based on the AFM detection of **P7**, we undertook the synthesis of this novel molecule to facilitate its unequivocal identification and quantification in *n*-decane's products by HPLC/UV/MS.

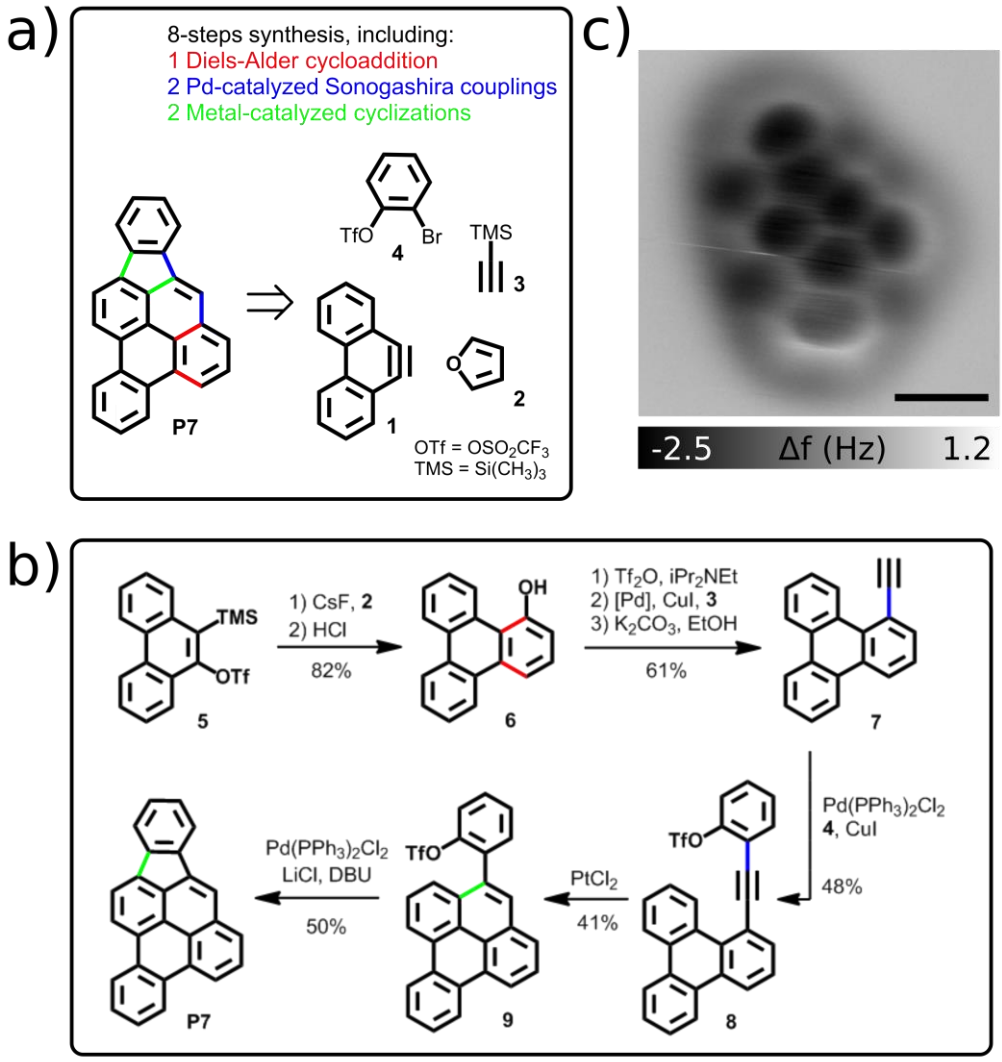


**Figure 2.** Synthesis of benz[*l*]indeno[1,2,3-*cd*]pyrene (**P7**): (a) Retrosynthetic analysis, (b) Synthetic route to **P7**, and (c) AFM image of the synthesized compound on Cu(111), confirming the successful preparation of **P7**. Scale bar is 5 Å.

Compound **P7** was prepared in eight steps based on the retrosynthetic analysis shown in Figure 2a. The synthesis was initiated by a Diels-Alder cycloaddition of aryne **1**, generated by fluoride-induced decomposition of triflate **5**, with furan **2** followed by acid treatment to obtain 1-triphenylenol **6** in 82% yield (Figure 2b).[68] Transformation of compound **6** into the corresponding triflate, followed by Pd-catalyzed Sonogashira coupling and base-induced desilylation afforded terminal alkyne **7** in 61% yield. Again, a Pd-catalyzed Sonogashira coupling between alkyne **7** and bromide **4** led to compound **8**, which was treated with $PtCl_2$ to induce a cycloisomerization to obtain triflate **9**.[69] Finally, Pd-catalyzed cyclization of compound **9** afforded **P7** in 50% yield (see supporting information for details). AFM measurements unequivocally confirmed the structure of the synthesized standard as benz[*l*]indeno[1,2,3-*cd*]pyrene (**P7**, Figure 2c), which is then used as reference standard for HPLC/UV/MS analysis.

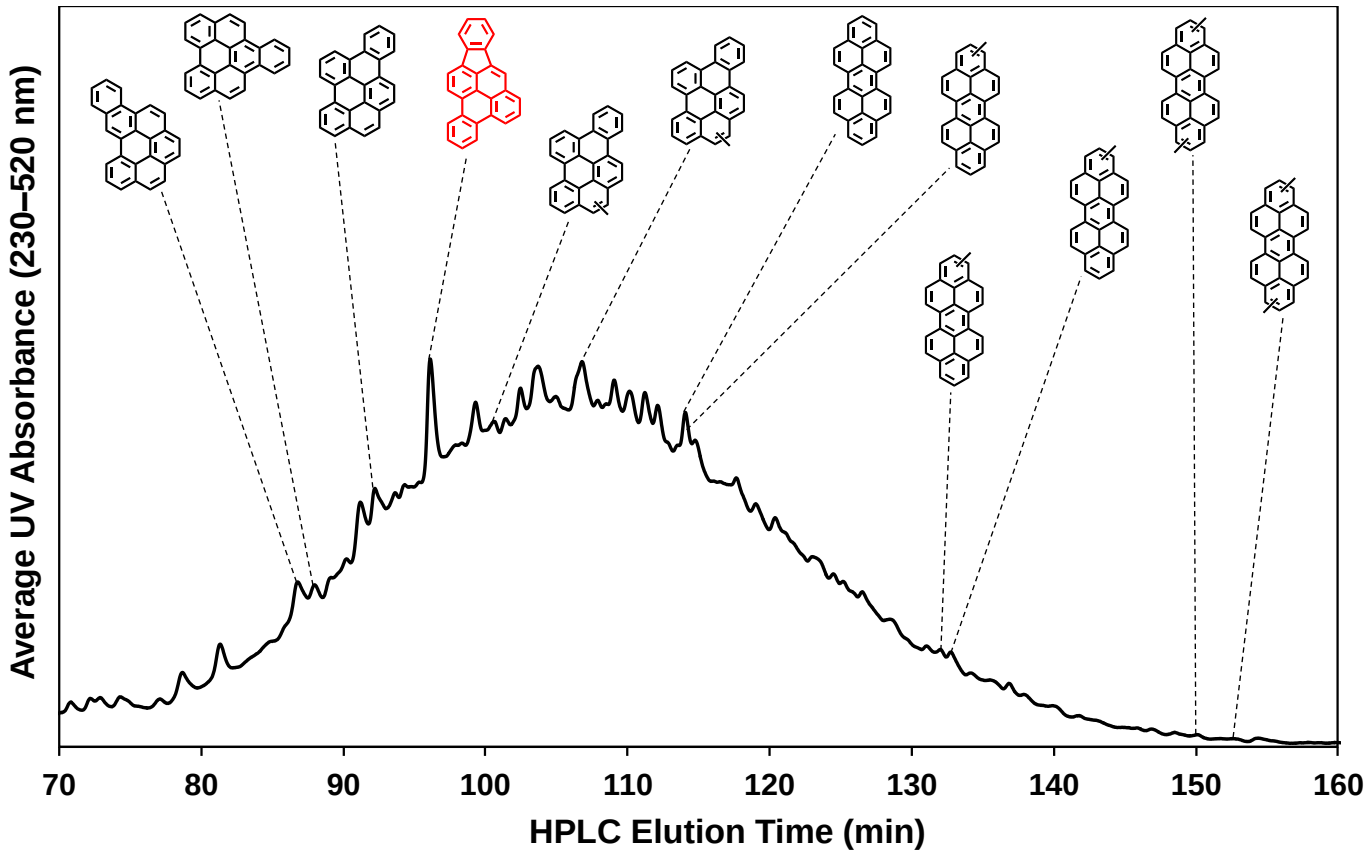


**Figure 3.** Reversed-phase HPLC chromatogram of Fraction **F** of the products of *n*-decane pyrolysis at 570 °C, 94.6 atm, and 133 sec. The 11 black structures, which include four unsubstituted $C_{26}H_{14}$

benzenoid PAH, five singly-methylated PAH, and two doubly-methylated (or ethylated) PAH are reported in literature.[33] The red structure corresponds to the newly identified PAH **P7**.

Normal-phase HPLC analysis of the standard of this newly synthesized $C_{26}H_{14}$ PAH **P7** reveals that it elutes in PAH-product Fraction **F** of *n*-decane pyrolysis, which mainly contains PAH with 13 π-bonds, *i.e.* $C_{26}H_{14}$ PAH and their alkylated derivatives.[32,33] By employing the reversed-phase HPLC method, which is used to analyze the Fraction **F**,[33] we determined that **P7** has a HPLC elution time of 96.1 min. This elution time corresponds to the single largest peak in the reversed-phase HPLC chromatogram of Fraction **F**, displayed in Figure 3. Previous HPLC analysis of Fraction **F** led to identification of 11 PAH (black structures in Figure 3).[33] However, due to the previous lack of a reference standard and/or UV spectrum that matched with the chromatographic peak eluting at 96.1 min in Fraction **F**, this HPLC peak was left unassigned. The mass spectrum of this unidentified PAH, shown in Figure 4a, eluting at the same time as **P7**, portrays the primary ion at 326, which corresponds to the molecular weight of a $C_{26}H_{14}$ PAH (same as **P7**). In Figure 4b, we present the UV spectrum of the unknown $C_{26}H_{14}$ PAH product of supercritical *n*-decane pyrolysis (in black), along with that of the synthesized standard of benz[*l*]indeno[1,2,3-*cd*]pyrene (**P7**, in red). Figure 4b displays the excellent agreement between the UV spectra of the product/standard pair, establishing the unequivocal identification of benz[*l*]indeno[1,2,3-*cd*]pyrene (**P7**) as a product of supercritical *n*-decane pyrolysis. The quantification of **P7** reveals that for *n*-decane pyrolysis experiments conducted at 570 °C, 94.6 atm, and 133 sec, this newly identified molecule accounts for 5.9% of the mass of Fraction **F**, which is equivalent to 0.267 μg of **P7** per g of *n*-decane fed to the reactor. Therefore, by employing AFM in conjunction with HPLC/UV/MS and synthetic chemistry, we established the exact structural identity of the novel seven-ring $C_{26}H_{14}$ PAH benz[*l*]indeno[1,2,3-*cd*]pyrene.

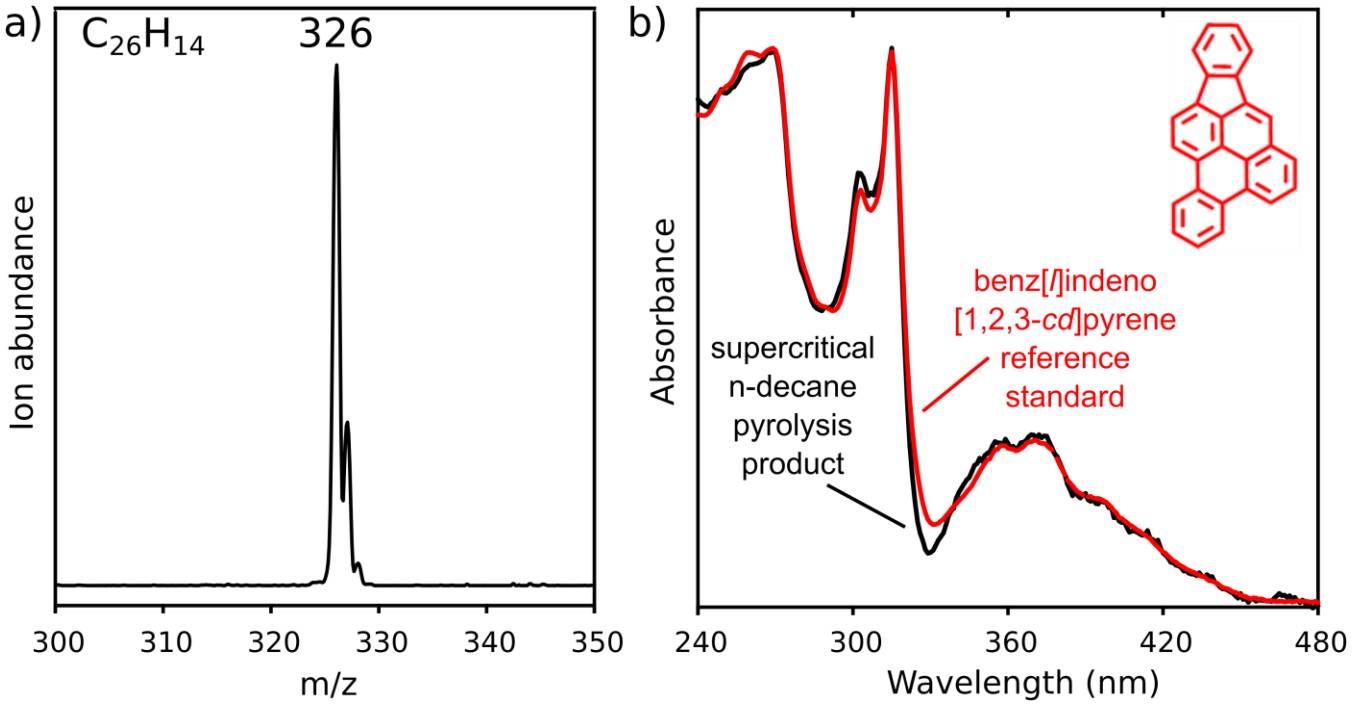


**Figure 4.** (a) Mass spectrum of the supercritical *n*-decane pyrolysis product, eluting at 96.1 min in the HPLC chromatogram in Figure 3; and (b) UV absorbance spectrum (in black) of the supercritical *n*-decane pyrolysis product, eluting at 96.1 min in the HPLC chromatogram in Figure 3, along with the UV absorbance spectrum (in red) of the reference standard of **P7**.

Because our HPLC analysis revealed that benz[*l*]indeno[1,2,3-*cd*]pyrene (**P7**) elutes in Fraction **F** of the products of *n*-decane pyrolysis, we further analyzed this PAH-product fraction by AFM to search for the presence of additional unknown PAH. The AFM images of six molecules measured in Fraction **F**, labelled **F1** to **F6**, along with tentatively assigned chemical structures are shown in Figure 5. The AFM measurements of Fraction **F** indicate that all of the imaged molecules have side groups attached to the PAH core and, expectedly, the most common side groups are methyl. Most of the molecules are seven-ring PAH, except for **F5** and **F6**, which contain eight and six rings, respectively. Each of these six PAH detected by AFM have an aromatic core that contains 13 π-bonds, which is consistent with our previous findings[32,33] that showed that Fraction **F** primarily contains PAH with 13 π-bonds. Three of these six molecules (**F1**, **F4**, and **F5**) have an aromatic core that corresponds to a $C_{26}H_{14}$ PAH. The aromatic cores of **F2** and **F3** correspond to $C_{27}H_{16}$ PAH and that of **F6** corresponds to a

$C_{26}H_{16}$ PAH. Although the aromatic cores of **F2**, **F3**, and **F6** constitute a slightly larger molecular formula than $C_{26}H_{14}$ they still contain 13 π-bonds, consistent with them eluting in Fraction **F**.[33]

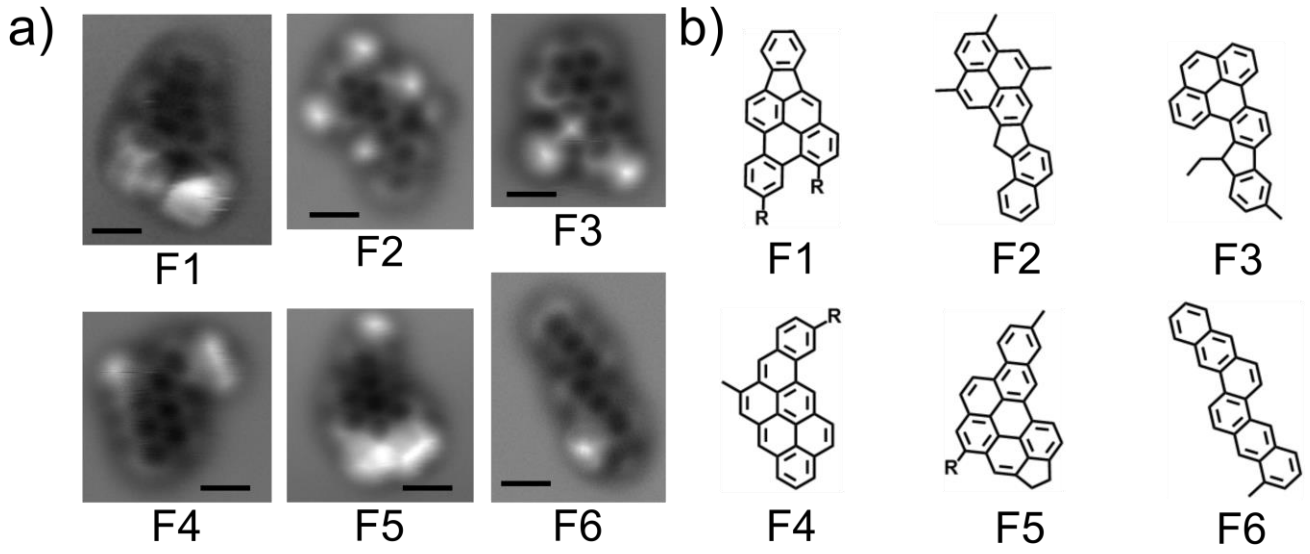


**Figure 5.** Fraction **F** of the products of *n*-decane pyrolysis at 570 °C, 94.6 atm, and 133 sec measured by AFM: (a) AFM measurements. Scale bars are 5 Å. **F4** and **F5** were measured on bilayer NaCl, all the other molecules were measured on Cu(111). (b) The PAH cores of the proposed chemical structures are benz[*l*]indeno[1,2,3-*cd*]pyrene (**F1**), benz[4,5]indeno[2,1-*a*]pyrene (**F2**), fluoreno[2,3-*e*]pyrene (**F3**), benz[*a*]anthanthrene (**F4)**, 4,5-dihydrodibenzo[*b,ghi*]cyclopenta[*lm*]perylene (**F5**), and dibenzo[*b,k*]-chrysene (**F6**).

**F1** is a substituted derivative of benz[*l*]indeno[1,2,3-*cd*]pyrene (**P7**), whose two side groups could not be identified. The bright appearance on the bottom right-hand side of the AFM image of **F1**, in Figure 5a, indicates a non-planar, bulky side-group at this position. Assignment of these groups might become possible in the future when more AFM characteristics for fingerprinting of molecular moieties will have been measured.[46,70] Of these six PAH shown in Figure 5, UV spectra and/or reference standards are available for benz[*l*]indeno[1,2,3-*cd*]pyrene, dibenzo[*b,ghi*]perylene, and dibenzo[*b,k*]chrysene, which correspond to the aromatic cores of **F1**, **F5**, and **F6**, respectively, but for none of their substituted counterparts. The reference standards or UV spectra of **F2**, **F3**, and **F4** and/or

their unsubstituted counterparts are unavailable to us. Therefore, it is certainly plausible that some of the unidentified peaks in the HPLC chromatogram of Fraction **F**, in Figure 3, could correspond to one or more of these novel PAH detected by AFM. The joint usage of STM orbital imaging with AFM can further aid in structure determination of unknown PAH in fuel-product mixtures, an example being **F4** (more details in the supporting information). In this case, the benz[*a*]anthanthrene motif is properly identified by comparing the experimentally obtained lowest unoccupied molecular orbital (LUMO) image with the calculated LUMO via density functional theory. This is the first time any of these six PAH have been reported as fuel pyrolysis and/or combustion products.

## 4. Conclusion

This study shows that an AFM-based strategy, in conjunction with synthetic chemistry and analytical tools, is advantageous for investigating molecular ensembles. We showcase the detection, identification, synthesis, and quantification of a novel seven-ring PAH product, benz[*l*]indeno[1,2,3-*cd*]pyrene, of supercritical *n*-decane pyrolysis. Aided by the AFM capability of probing single molecules, even at lower concentrations than 1 ppm, novel molecules within fuel pyrolysis products were reported. The demonstrated multi-disciplinary approach directs the production of chemical standards in a cost-effective and time-saving manner and should generally be applicable in fields where a diverse range of PAH are being formed.

## 5. Acknowledgments

We thank Rolf Allenspach for comments on the manuscript. We are also grateful to Dr. Arthur Lafleur and Ms. Elaine Plummer, of the Massachusetts Institute of Technology; Dr. John Fetzer, FETZPAHS; and Dr. Werner Schmidt, PAH-Forschung, for providing reference standards and UV spectra of PAH. The authors acknowledge financial support by the European Research Council (Advanced grant ‘CEMAS’ – agreement no. 291194 and Consolidator grant ‘AMSEL’ – agreement no. 682144), EU projects ‘PAMS’ (Contract no. 610446) and Initial training network ‘ACRITAS’ (Contract

no. 317348), the Air Force Office of Scientific Research (Grant FA9550-13-1-0172), the Spanish Agencia Estatal de Investigación (MAT2016-78293-C6-3-R and CTQ2016-78157-R), the Xunta de Galicia (Centro singular de investigación de Galicia accreditation 2016-2019, ED431G/09), and the European Regional Development Fund (ERDF).

Supplementary Material: Additional AFM measurements, chemical structures, and synthetic procedures.

**References**

[1] Fetzer, J. C. *Polycyclic Aromat. Compd.* **2007**, *27*, 143–162.

[2] Harvey, R. G. *Polycyclic Aromatic Hydrocarbons: Chemistry and Carcinogenicity*; John Wiley & Sons; 1997.

[3] Marvin, C. H.; Smith, R. W.; Bryant, D. W.; McCarry, B. E. *J. Chromatogr. A.* **1999**, *863*, 13–24.

[4] Schmidt, W.; Grimmer, G.; Jacob, J.; Dettbarn, G.; Naujack, K. W. *Fresenius Z. Anal. Chem.* **1987**, *326*, 401–413.

[5] Wornat, M. J.; Sarofim, A. F.; Lafleur, A. L. *Proc. Combust. Inst.* **1992**, *24*, 955–963.

[6] Peaden, P.A.; Lee, M.L.; Hirata, Y.; Novotny, M. *Anal. Chem.* **1980**, *52*, 2268–2271.

[7] Wilson, W. B.; Hayes, H. V.; Sander, L. C.; Campiglia, A. D.; Wise, S. A. *Anal. Bioanal. Chem.* **2017**, *409*, 5171–5183.

[8] Fetzer, J. C. *Large (C≥24) Polycyclic Aromatic Hydrocarbons: Chemistry and Analysis*; John Wiley & Sons; 2000.

[9] Dias, J. R. *Polycyclic Aromat. Compd.* **2014**, *34*, 177–190.

[10] Zander, M. *Polycyclic Aromat. Compd.* **1995**, *7*, 209–221.

[11] Haynes, B. S.; Wagner, H. G. *Prog. Energy Combust. Sci.* **1981**, *7*, 229–273.

[12] Wornat, M. J.; Sarofim, A. F.; Longwell, J. P. *Energy Fuels* **1987**, *1*, 431–437.

[13] Richter, H.; Howard, J. B. *Prog. Energy Combust. Sci.* **2000**, *26*, 565–608.

[14] Pope, C. A., III; Burnett, R. T.; Thun, M. J.; Calle, E. E.; Krewski, D.; Ito, K.; Thurston, G. D. *J. Am. Med. Assoc.* **2002**, *287*, 1132–1141.

[15] Nel, A. *Science* **2005**, *308*, 804–806.

[16] Kennedy, I. M. *Proc. Combust. Inst.* **2007**, *31*, 2757–2770.

[17] Jacobson, M. Z. *Nature* **2001**, *409*, 695–697.

[18] Service, R. F. *Science* **2008**, *319*, 1745.

[19] Bond, T. C.; Doherty, S. J.; Fahey, D. W.; Forster, P. M.; Berntsen, T.; DeAngelo, B. J.; Flanner, M. G.; Ghan, S.; Kärcher, B.; Koch, D.; Kinne, S. *J. Geophys. Res. D: Atmos.* **2013**, *118*, 5380–5552.

[20] Shah, N.; Panjala, D.; Huffman, G. P. *Energy Fuels* **2001**, *15*, 1528–1534.

[21] Xu, X.; Pacey, P. D. *Phys. Chem. Chem. Phys*. **2005**, *7*, 326–333.

[22] Fu, P. P.; Beland, F. A.; Yang, S. K. *Carcinogenesis* **1980**, *1*, 725–727.

[23] Grimmer G. *Environmental Carcinogens: Polycyclic Aromatic Hydrocarbons*; CRC Press; Boca Raton, FL; 1983.

[24] Durant, J. L.; Busby Jr, W. F.; Lafleur, A. L.; Penman, B. W.; Crespi, C. L. *Mutat. Res.* **1996**, *371*, 123–157.

[25] Edwards, T. *Combust. Sci. Technol.* **2006**, *178*, 307–334.

[26] Andrésen, J. M.; Strohm, J. J.; Sun, L.; Song, C. *Energy Fuels* **2001**, *15*, 714–723.

[27] DeWitt, M. J.; Edwards, T.; Shafer, L.; Brooks, D.; Striebich, R.; Bagley, S. P.; Wornat, M. J. *Ind. Eng. Chem. Res.* **2011**, *50*, 10434–10451.

[28] Kalpathy, S. V.; Poddar, N. B.; Bagley, S. P.; Wornat, M. J. *Proc. Combust. Inst.* **2015**, *35*, 1833–1841.

[29] Kalpathy, S. V.; Bagley, S. P.; Wornat, M. J. *Ind. Eng. Chem. Res.* **2015**, *54*, 7014–7027.

[30] Kalpathy, S. V., Poddar, N. B., Hurst, E. A., Caspary, E. C., Wornat, M. J. *Proc. Combust. Inst.* **2017**, *36*, 965–973.

[31] Heneghan, S. P.; Zabarnick, S.; Ballal, D. R.; Harrison, W. E., III. *J. Energy Res. Technol.* **1996**, *118*, 170–179.

[32] Bagley, S. P.; Wornat, M. J. *Energy Fuels* **2011**, *25*, 4517–4527.

[33] Bagley, S. P.; Wornat, M. J. *Energy Fuels* **2013**, *27*, 1321–1330.

[34] Edwards, T. *J. Propul. Power* **2003**, *19*, 1089–1107.

[35] Lai, W. C.; Song, C. *Fuel* **1995**, *74*, 1436–1451.

[36] Gross, L., Mohn, F., Moll, N., Liljeroth, P., and Meyer, G. *Science* **2009**, 325, 1110–1114.

[37] Gross, L., Mohn, F., Moll, N., Meyer, G., Ebel, R., Abdel-Mageed, W. M., and Jaspars, M. *Nat. Chem.* **2010**, 2, 821–825.

[38] Hanssen, K. O., Schuler, B., Williams, A., Demissie, T. B., Hansen, E., Andersen, J. H., Svenson, J., Blinov, K., Repisky, M., Mohn, F., Meyer, G., Svendsen, J.-S., Ruud, R., Elyashberg, M., Gross, L., Jaspars, M., and Isaksson, J. *Angew. Chem. Int. Ed.* **2012**, 51, 12238–12241.

[39] Schuler, B., Collazos, S., Gross, L., Meyer, G., Pérez, D., Guitián, E., and Peña, D. *Angew. Chem. Int. Ed.* **2014**, 126, 9150–9152.

[40] de Oteyza, D. G., Gorman, P., Chen, Y.-C., Wickenburg, S., Riss, A., Mowbray, D. J., Etkin, G., Pedramrazi, Z., Tsai, H.-Z., Rubio, A., Crommie, M. F., and Fischer, F. R. *Science* **2013**, 340, 1434–1437.

[41] Schuler, B., Meyer, G., Peña, D., Mullins, O. C., and Gross, L. *J. Am. Chem. Soc.* **2015**, 137, 9870–9876.

[42] Stetsovych, O., Švec, M., Vacek, J., Chocholoušová, J. V., Jancark, A., Rybácek, J., Kosmider, K., Stará, I. G., Jelnek, P., and Stary, I. *Nat. Chem.* **2017**, 9, 213–218.

[43] Riss, A., Paz, A. P., Wickenburg, S., Tsai, H.-Z., De Oteyza, D. G., Bradley, A. J., Ugeda, M. M., Gorman, P., Jung, H. S., Crommie, M. F., Rubio, A., and Fischer, F. R. *Nat. Chem.* **2016**, 8, 678–683.

[44] Kawai, S., Haapasilta, V., Lindner, B. D., Tahara, K., Spijker, P., Buitendijk, J. A., Pawlak, R., Meier, T., Tobe, Y., Foster, A. S., et al. *Nat. Comm.* **2016**, **7**, 12711–12717.

[45] Schulz, F., Jacobse, P. H., Canova, F. F., van der Lit, J., Gao, D. Z., van den Hoogenband, A., Han, P., Gebbink, R. J. M. K., Moret, M. E., Joensuu, P. M., Swart, I., Liljeroth, P. *J. Phys. Chem. C.* **2017**, 121, 2896–2904.

[46] Schuler, B., Fatayer, S., Meyer, G., Rogel, E., Moir, M., Zhang, Y., Harper, M. R., Pomerantz, A. E., Bake, K. D., Witt, M., et al. *Energy Fuels* **2017**, 31, 6856–6861.

[47] Schuler, B., Liu, W., Tkatchenko, A., Moll, N., Meyer, G., Mistry, A., Fox, D., Gross, L. *Phys. Rev. Lett.* **2013**, 111, 106103–106107.

[48] Schuler, B., Zhang, Y., Collazos, S., Fatayer, S., Meyer, G., Pérez, D., Guitián, E., Harper, M. R., Kushnerick, J. D., Peña, D., Gross, L. *Chem. Sci.* **2017**, 8, 2315–2320.

[49] Wise, S. A.; Chesler, S. N.; Hertz, H. S.; Hilpert, L. R.; May, W. E. *Anal. Chem*. **1977**, *49*, 2306–2310.

[50] Giessibl, F. J. *Appl. Phys. Lett.* **1999**, 73, 3956–3958.

[51] Albrecht, T. R., Grütter, P., Horne, D., and Rugar, D. *J. Appl. Phys.* **1991**, 69, 668–673.

[52] Bennewitz, R., Barwich, V., Bammerlin, M., Loppacher, C., Guggisberg, M., Baratoff, A., Meyer, E., and Güntherodt, H.-J. *Surf. Sci.* **1999**, 438, 289–296.

[53] Bartels, L., Meyer, G., and Rieder, K.-H. *Appl. Phys. Lett.* **1997**, 71, 213–215.

[54] van der Heijden, N. J., Hapala, P., Rombouts, J. A., van der Lit, J., Smith, D., Mutombo, P., Svec, M., Jelinek, P., and Swart, I. *ACS Nano* **2016**, 10, 8517–8525.

[55] Gross, L., Mohn, F., Moll, N., Schuler, B., Criado, A., Guitián, E., Peña, D., Gourdon, A., and Meyer, G. *Science* **2012**, 337, 1326–1329.

[56] Hapala, P., Kichin, G., Wagner, C., Tautz, F. S., Temirov, R., and Jelínek, P. *Phys. Rev. B* **2014**, 90, 085421.

[57] Albrecht, F., Pavliček, N., Herranz-Lancho, C., Ruben, M., and Repp, J. *J. Am. Chem. Soc.* **2015**, *137* (23), 7424-7428.

[58] Moreno, C., Stetsovych, O., Shimizu, T. K., and Custance, O. *Nano Letters* **2015** *15* (4), 2257-2262.

[59] Majzik, Z., Cuenca, A. B., Pavliček, N., Miralles, N., Meyer, G., Gross, L., and Fernández, E. *ACS Nano* **2016** *10* (5), 5340-5345.

[60] Hinaut, A., Meier, T., Pawlak, R., Feund, S., Jöhr, R., Kawai, S., Glatzel, T., Decurtins, S., Müllen, K., Narita, A., Liu, S.-X., Meyer, E. *Nanoscale* **2018**, *10* (3), 1337–1344.

[61] Hamann, C.; Woltmann, R.; Hong, I.-P.; Hauptmann, N.; Karan, S.; Berndt, R. *Rev. Sci. Instrum.* **2011**, *82* (3), 33903.

[62] Rauschenbach, S.; Stadler, F. L.; Lunedei, E.; Malinowski, N.; Koltsov, S.; Costantini, G.; Kern, K. Electrospray Ion Beam Deposition of Clusters and Biomolecules. *Small* **2006**, *2* (4), 540–547.

[63] Gross, L.; Schuler, B.; Pavliček, N.; Fatayer, S.; Majzik, Z.; Moll, N.; Peña, D.; Meyer, G. *Angew. Chem. Int. Ed.* **2018**, *57* (15), 3888–3908.

[64] Houlton, P. R.; Kemp, W. *Tetrahedron Lett.* **1968**, *9*, 4093–4096.

[65] Lang, K. F.; Buffleb, H.; Kalowy, J. *Chem. Ber.* **1961**, *94*, 523–526.

[66] Ajaz, A.; Voukides, A. C.; Cahill, K. J.; Thamatam, R.; Skraba-Joiner, S. L.; Johnson, R. P. *Aust. J. Chem.* **2014**, *67*, 1301–1308.

[67] Jackson, E. A.; Xue, X.; Cho, H. Y.; Scott, L. T. *Aust. J. Chem.* **2014**, *67*, 1279–1287.

[68] Pérez, D.; Peña, D.; Guitián, E. *Eur. J. Org. Chem.* **2013**, *27*, 5981–6013.

[69] Wu, D.; Zhang, H.; Liang, J.; Ge, H.; Chi, C.; Wu, J.; Liu, S. H.; Yin, J. *J. Org. Chem.* **2012**, *77*, 11319–11324.

[70] Pavlicek, N. and Gross, L. *Nat. Rev. Chem.* **2017**, 1, 0005, 1–11.

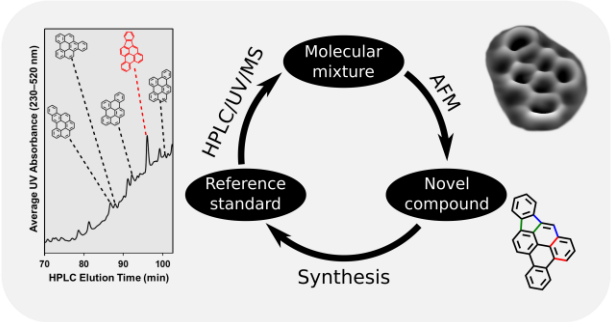


**For Table of Contents Only**

# Supplemental Information

**Atomic force microscopy identifying fuel pyrolysis products and directing the synthesis of analytical standards**

## CONTENTS

## 1. AFM Characterization

### 1.1.Additional AFM measurements of Fraction **P**

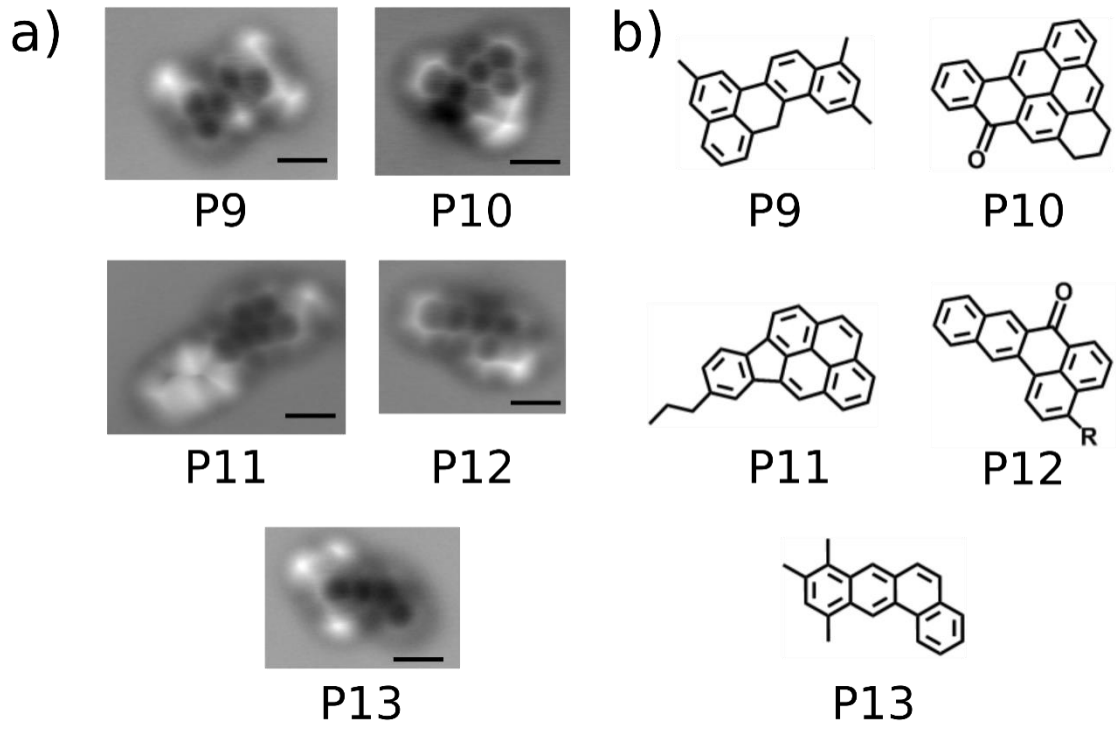


**Figure S1.** Additional AFM measurements of Fraction **P** of the products of *n*-decane pyrolysis at 570 °C, 94.6 atm, and 133 sec: (a) Constant-height AFM measurements with a CO- functionalized tip. Scale bars are 5 Å. All moleculeswere measured on Cu(111).(b) Proposed chemical structures measured in (a).(Note: Supercritical *n*-decane pyrolysis does not produce any oxygen-containing species because we take precautions to ensure that oxygen is not present and/or introduced in the reaction environment. Molecules **P10** and **P12** contain CO groups that result from the oxidation of the corresponding methylene groups[1,2] when the *n*-decane-pyrolysis product fractions get exposed to air and light during the sample preparation procedure.)

[1] Ramdahl, T. *Environ. Sci. Technol.* **1983**, *17*, 666–670.

[2]Streitwieser, A., Jr.; Word, J. M.; Guibe, F.; Wright, J. S. *J. Org. Chem.***1981**, *46*, 2588–2589.

1.2.Common motifs of Fraction **P**

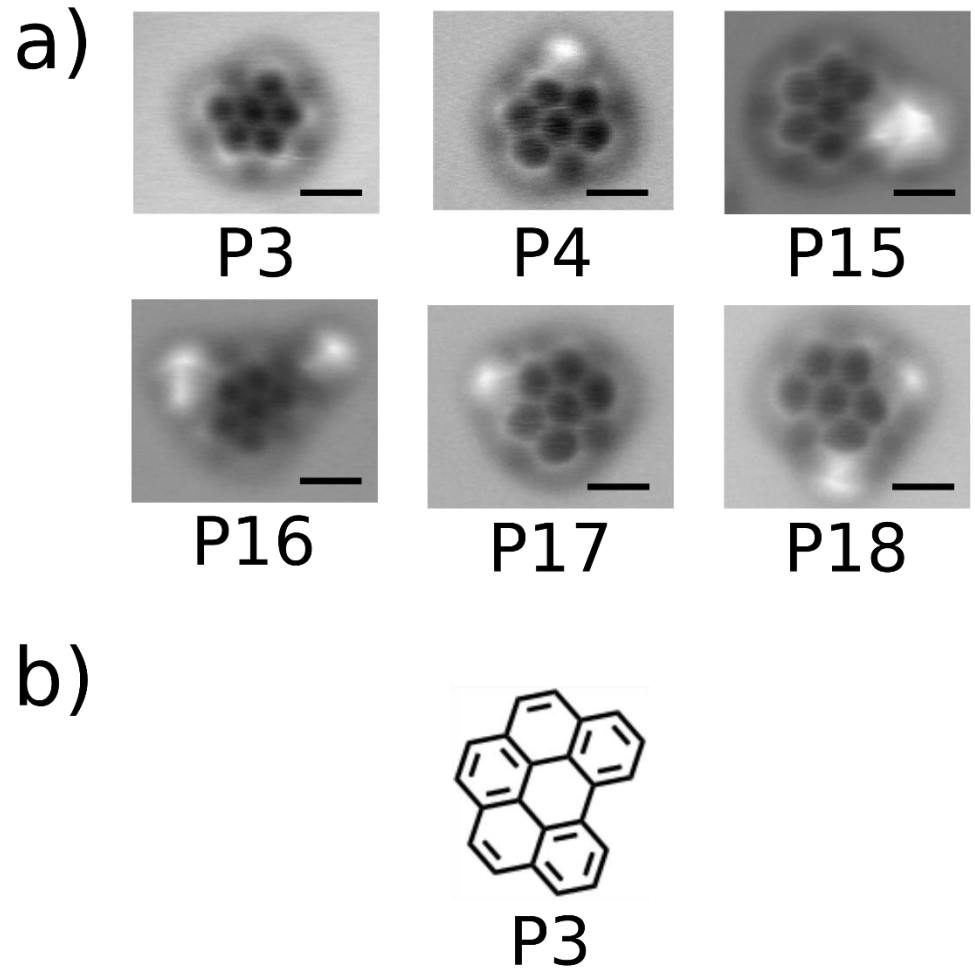


**Figure S2.** Common motifs found in Fraction **P** of the products of *n*-decane pyrolysis at 570 °C, 94.6 atm, and 133 sec: (a) AFM images of benzo[*ghi*]perylene (**P3**) and its methylated derivatives (**P4** and **P15–P18**) and (b) the chemical structure of benzo[*ghi*]perylene.

1.3.Molecular orbital imaging and calculation for **F4**

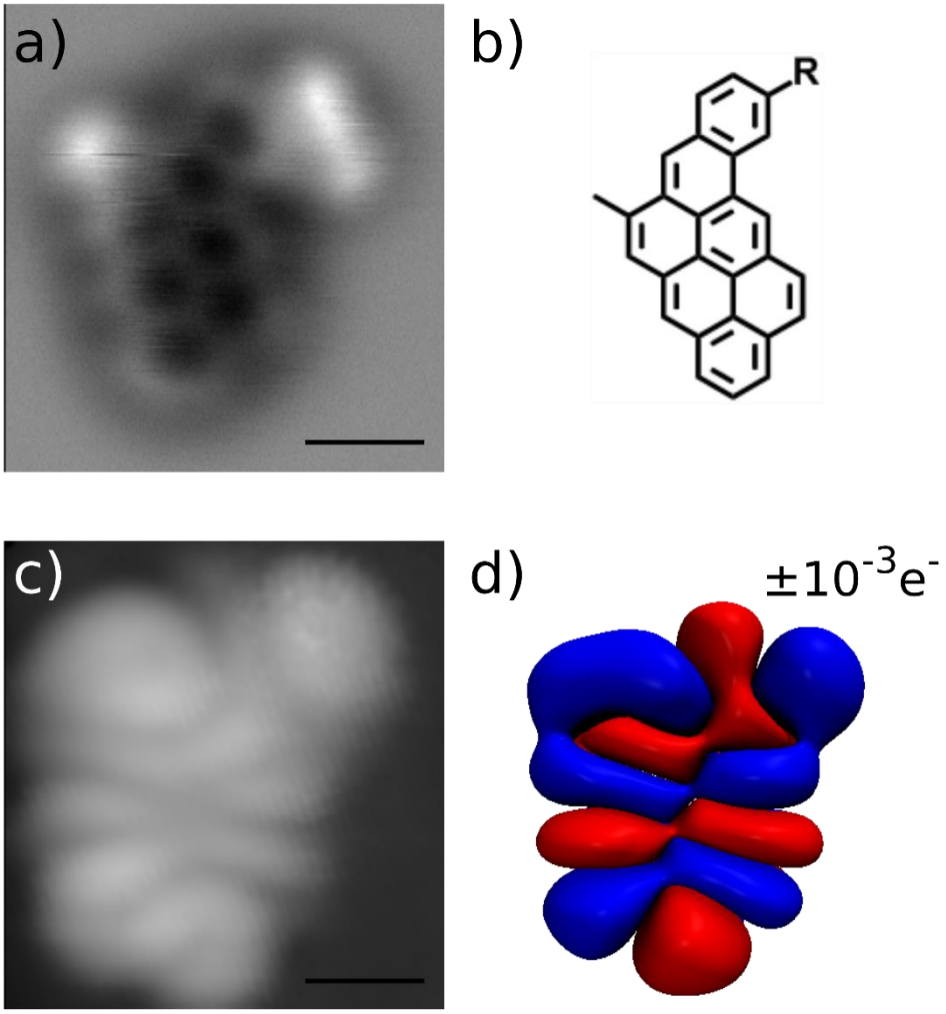


**Figure S3. F4** orbital imaging and calculation: (a) AFM image of **F4** on bilayer NaCl, (b) Structural model of **F4**, (c) STM image of the negative ion resonance of **F4** at 1.6 V, and (d) DFT calculation of the LUMO orbital of the structure in panel b, without the R group.

## 2. General methods for the synthesis of P7

All reactions were carried out under argon using oven-dried glassware. TLC was performed on Merck silica gel 60 F254; chromatograms were visualized with UV light (254 and 360 nm). Flash column chromatography was performed on Merck silica gel 60 (ASTM 230-400 mesh). $^{1}$H and $^{13}$C NMR spectra were recorded at 300 and 75 MHz, 400 and 101 MHz or750 and 188 MHz (Varian Mercury 300, Varian Inova-400 or Varian Inova-750 instruments, respectively). Low-resolution electron impact mass spectra were determined at 70 eV on a HP-5988A instrument. High-resolution mass spectra (HRMS) were obtained on a Micromass Autospec spectrometer. UV/Vis spectra were obtained on a Jasco V-530 spectrophotometer.

Triflates**5**[1]and **4**[2]were prepared following published procedures (Figure S1).Commercial reagents and anhydrous solvents were purchased from ABCR GmbH, Aldrich Chemical Co., or Strem Chemicals Inc., and were used without further purification.

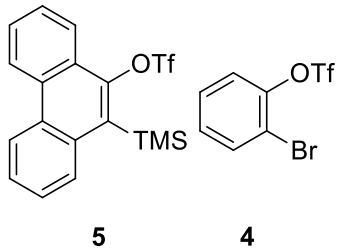


**Figure S4.** Molecular structure of triflates **4** and **5**.

## 3. Experimental details and spectroscopic data

### 3.1. Synthesis of1,4-dihydro-1,4-epoxytriphenylene (**10**)

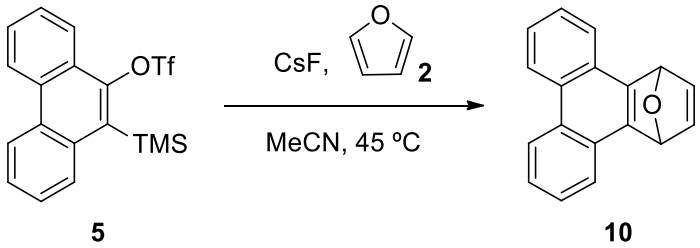


**Figure S5.** Synthesis of compound **10**.

A sealed tube was charged with triflate **5** (300 mg, 0.75 mmol) and furan (**2**, 0.55 mL, 7.5 mmol). The mixture was dissolved in MeCN (7.5 mL), anhydrous CsF (342 mg, 2.25 mmol) was added andthe mixture was heated at 45°C under argon for 12 h. Then, $H_2O$ (10 mL) and $Et_2O$ (10 mL) were added, the phases were separated and the aqueous layer was extracted with $Et_2O$ (2 x 10 mL). The combined organic layers were dried over anhydrous $Na_2SO_4$, filtered, and concentrated under reduced pressure. The residue was purified by column chromatography ($SiO_2$, Hexane/$CH_2Cl_2$ 3:1) to afford **10** (150 mg, 82%) as a yellow solid. $^1$H NMR (298 K, 300 MHz, $CDCl_3$) δ: 8.80 – 8.70 (m, 2H), 8.03 – 7.91 (m, 2H), 7.73 – 7.59 (m, 4H), 7.30 (s, 2H), 6.43 (s, 2H) ppm.[3]

### 3.2. Synthesis of triphenylen-1-ol (**6**)

[1] Peña, D.; Cobas, A.; Pérez, D.; Guitián, E. *Synthesis***2002**, 1454.

[2] Ma, Y.; Zhang, H.-Y.; Yang, S.-D.*Org. Lett.***2015**, *17*, 2034.

[3] Romero, C.; Peña, D.; Pérez, D.; Guitián, E. *J. Org. Chem*. **2008**, *73*, 7996.

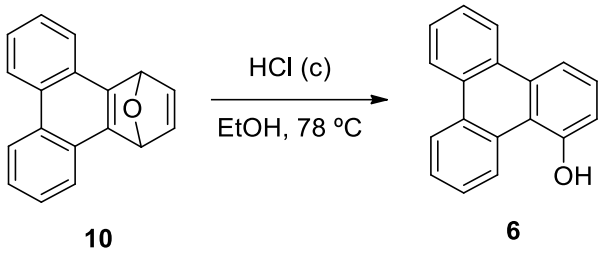


**Figure S6.** Synthesis of compound **6**.

Concentrated aqueous HCl solution (36%, 3 mL) was added to a solution of **10** (150mg,0.61 mmol) in EtOH (12 mL), and the mixture was stirred at 78 ºC for 2h. Then, this mixture was cooled to room temperature, $H_2O$ (5 mL) and $Et_2O$ (10 mL) were added, the phases were separated, and the aqueous layer was extracted with $Et_2O$ (3 x 10 mL). The combined organic layers were dried over anhydrous $Na_2SO_4$, filtered, and concentrated under reduced pressure. The residue was purified by column chromatography ($SiO_2$, Hexane/$Et_2O$ 7:3) to afford **6** (150 mg, 100%) as a white solid. $^1$H NMR (298 K, 300 MHz, $CDCl_3$) δ: 9.69 – 9.55 (m, 1H), 8.74 – 8.57 (m, 3H), 8.31 (dd, *J* = 8.4, 1.1 Hz, 1H), 7.71 – 7.57 (m, 4H), 7.49 (t, *J* = 8.0 Hz, 1H), 7.02 (dd, *J* = 7.7, 1.1 Hz, 1H), 5.62 (s, 1H) ppm.[3]

## 3.3. Synthesis of triphenylen-1-yl trifluoromethanesulfonate (**11**)

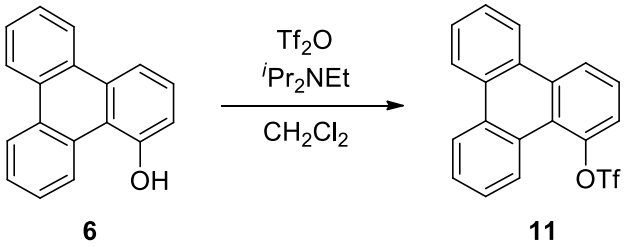


**Figure S7.** Synthesis of compound **11**.

To a solution of triphenylen-1-ol (**6**, 140 mg, 0.57 mmol) and$^i$Pr$_2$NEt (96 µL, 0.57 mmol) in anhydrous $CH_2Cl_2$ (4 mL) $Tf_2O$ (191 µL, 1.14 mmol) was added dropwise at 0 ºC over 30 min. The mixture was stirred at room temperature for 2 h and saturated aqueous $NaHCO_3$ (10 mL) was added. The organic layer was separated and the aqueous layer was extracted with $CH_2Cl_2$ (3x 10 mL). The combined organic layers were dried over anhydrous $Na_2SO_4$, filtered and concentrated under reduced pressure. The crude product was purified by column chromatography ($SiO_2$, Hexane/$Et_2O$/$CH_2Cl_2$ 8.5:2:0.5) to afford compound **11** (171 mg, 80%) as a white solid. $^1$H NMR (298 K, 300 MHz, $CDCl_3$) δ: 9.02 (dd, *J* = 7.8, 1.9 Hz, 1H), 8.72 – 8.46 (m, 4H), 7.81 – 7.50 (m, 6H) ppm.$^{13}$C NMR (298 K, 75 MHz, $CDCl_3$) δ: 147.4 (C), 133.5 (C), 131.1 (C), 130.4 (C), 128.7 (C), 128.5 (CH), 128.5 (CH), 128.3 (CH), 127.9 (CH), 127.3 (CH), 126.9 (CH), 126.6 (C), 123.8 (CH), 123.7 (C), 123.6 (CH), 123.6 (CH), 123.5 (CH), 121.6 (CH) 118.7 (q, *J* = 321.0 Hz, $CF_3$) ppm. MS (EI), *m/z* (%): 376 (100), 244 (30), 215 (25). HRMS (EI) for $C_{19}H_{11}O_3F_3S$, calculated: 376.0370, found: 376.0381.

## 3.4. Synthesis of trimethyl(triphenylen-1-ylethynyl)silane (**12**)

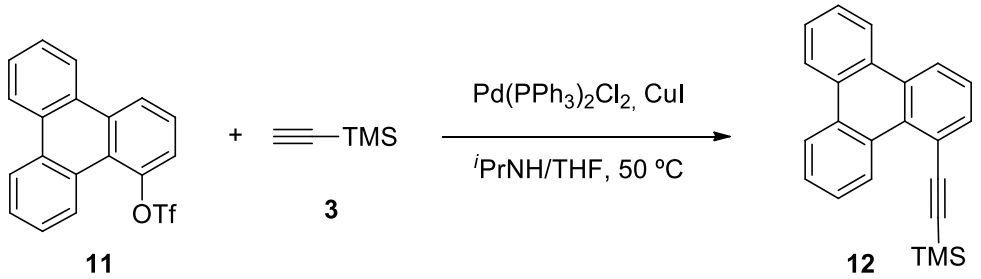


**Figure S8.** Synthesis of compound **12**.

To a deoxygenatedsolution of triflate **11** (120 mg, 0.32 mmol), $Pd(PPh_3)Cl_2$ (11.2 mg, 0.016 mmol) and CuI (1.2 mg, 0.006 mmol) in $^{i}$PrNH/THF (1:1, 3.5 mL) ethynyltrimethylsilane (**3**, 136 µL, 0.96 mmol) was added and the resulting mixture was heated at 50 ºC for 16 h. The solvent was evaporated under reduced pressure and the crude product was purified by column chromatography ($SiO_2$, Hexane) to afford trimethyl(triphenylen-1-ylethynyl)silane (**12**, 103 mg, 99%) as a white solid. $^{1}$H NMR (298 K, 300 MHz, $CDCl_3$) δ: 10.28 (dd, *J* = 8.5, 1.3 Hz, 1H), 8.74 – 8.53 (m, 4H), 7.91 (dd, *J* = 7.4, 1.6 Hz, 1H), 7.64 (m,5H), 0.37 (s, 9H) ppm. $^{13}$C NMR (298 K, 75 MHz, $CDCl_3$) δ: 136.0 (CH), 130.9 (C), 130.6 (C), 130.5 (C), 130.1 (C), 129.8 (C), 129.7 (C), 127.8 (CH), 127.7 (CH), 127.6 (CH), 127.3 (CH), 126.0 (CH), 125.8 (CH), 124.1 (CH), 123.6 (CH), 123.2 (CH), 122.9 (CH), 119.6 (C), 108.3 (C), 100.4 (C), 0.0 ($3CH_3$)ppm. MS (EI), *m/z* (%): 324 (64), 309 (100), 293 (16), 279 (12). HRMS (EI) for $C_{23}H_{20}Si$, calculated: 324.1334, found: 324.1345.

## 3.5. Synthesis of 1-ethynyltriphenylene (**7**)

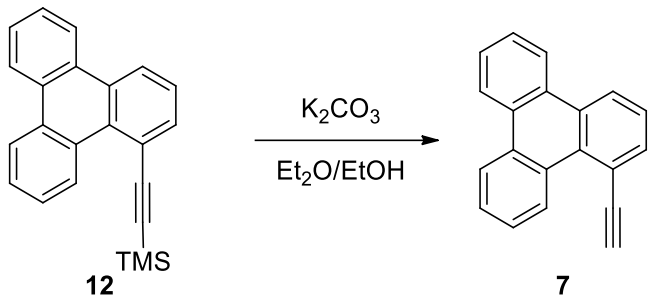


**Figure S9.** Synthesis of compound **7**.

To a solution of trimethyl(triphenylen-1-ylethynyl)silane (**12**, 90 mg, 0.28 mmol) in $Et_2O$/EtOH (1:1, 3 mL) $K_2CO_3$(115 mg, 0.84 mmol) was added. The mixture was stirred at room temperature for 4 h. The solvent was evaporated under reduced pressure, and the residue was mixed with 5 mL of satured aqueous $NaHCO_3$ and extracted with $Et_2O$ (3 x 10 mL). The combined organic layers were dried over anhydrous $Na_2SO_4$, filtered and concentrated under reduced pressure. The crude product was purified by column chromatography ($SiO_2$, Hexane) to afford compound **7** (53 mg, 76%) as a white solid. $^1$H NMR (300 MHz, $CDCl_3$) δ: 10.21 (dd, *J* = 7.2, 2.5 Hz, 1H), 8.67 – 8.47 (m, 4H), 7.95 (dd, *J* = 7.4, 1.4 Hz, 1H), 7.76 – 7.47 (m, 5H), 3.67 (s, 1H) ppm. $^{13}$C NMR (298 K, 75 MHz, $CDCl_3$) δ: 136.5 (CH), 130.9 (C), 130.7 (C), 130.6 (C), 130.1 (C), 129.6 (2C), 127.8 (CH), 127.6 (CH), 127.4 (2CH), 126.1 (CH), 126.1 (CH), 124.3 (CH), 123.5 (CH), 123.2 (CH), 123.0 (CH), 118.6 (C), 86.5 (C), 83.2 (CH) ppm. MS (EI), *m/z* (%): 252 (100), 239 (8). HRMS (EI) for $C_{20}H_{12}$, calculated: 252.0939, found: 252.0933.

## 3.6. Synthesis of 2-(triphenylen-1-ylethynyl)phenyltrifluoromethanesulfonate (**8**)

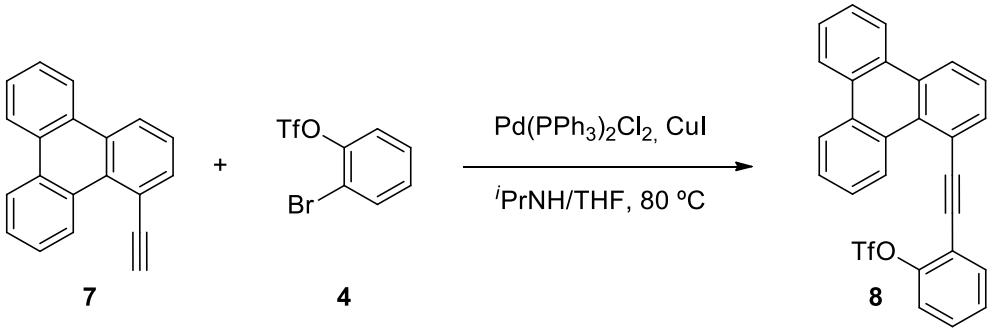


**Figure S10.** Synthesis of compound **8**.

To a deoxygenated solution of 2-bromophenyl trifluoromethanesulfonate (**4**, 51 mg, 0.167 mmol), $Pd(PPh_3)_2Cl_2$ (5.9 mg, 0.008 mmol) and CuI (1.6 mg, 0.008 mmol) in $^i$PrNH/THF (1:1, 2 mL) 1-ethynyltriphenylene (**7**, 50 mg, 0.20 mmol) was added and the resulting mixture was heated at 80 °C for 16 h. The solvent was evaporated under reduced pressure and the crude product was purified by column chromatography ($SiO_2$, Hexane/$CH_2Cl_2$ 9:1) to afford compound **8** (42 mg, 48%) as a yellow solid. $^1$H NMR (298 K, 300 MHz, $CDCl_3$) δ:10.05 (d, *J* = 8.1 Hz, 1H), 8.75 – 8.52 (m, 4H), 8.06 (d, *J* = 7.4 Hz, 1H), 7.79 – 7.56 (m, 6H), 7.51 – 7.33 (m, 3H) ppm. $^{13}$C NMR (298 K, 75 MHz, $CDCl_3$) δ: 149.7 (C), 135.7 (CH), 133.8 (CH), 131.1(C), 130.8 (C), 130.6 (C), 130.2 (C), 129.9 (CH), 129.7 (2C), 128.4 (CH), 128.0 (CH), 127.8 (CH), 127.5 (2CH), 126.4 (CH), 126.3 (CH), 124.7 (CH), 123.7 (CH), 123.3 (CH), 123.1 (CH), 121.9 (CH), 118.9 (C), 118.8 (C), 99.2 (C), 87.5 (C) 118.9 (q, *J* = 321.4 Hz, $CF_3$).MS (EI), *m/z* (%): 476 (83), 343 (100), 315 (70). HRMS (EI) for $C_{27}H_{15}O_3F_3$, calculated: 476.0694, found: 476.0704.

3.7. Synthesis of2-(benzo[*e*]pyren-4-yl)phenyltrifluoromethanesulfonate (**9**)

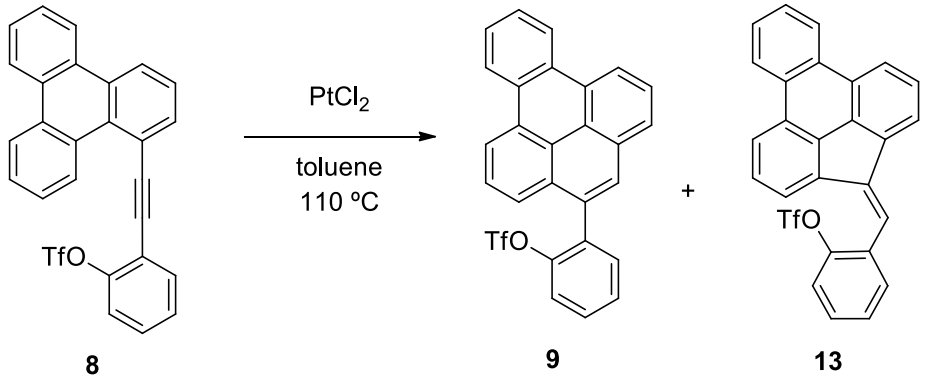


**Figure S11.** Synthesis of compound **9**.

A sealed tube was charged with triflate **8** (38 mg, 0.08 mmol) and $PtCl_2$ (127 mg, 0.48 mmol). The mixture was dissolved in toluene (4 mL) and heated at 110°C for 16h. The solvent was concentrated under reduced pressure and the residue was purified by column chromatography ($SiO_2$, Hexane/$CH_2Cl_2$ 9:1) to afford compounds **13**(19 mg, 49%) and **9**(16 mg, 41%) as yellow solids.

**Compound 13**:$^1$H NMR (298 K, 400 MHz, $CDCl_3$) δ: 8.65 – 8.55 (m, 2H), 8.33 (d, *J* = 8.0 Hz, 1H), 8.28 (d, *J* = 7.5 Hz, 1H), 7.97 (dd, *J* = 7.1, 2.1 Hz, 1H), 7.93 (d, *J* = 7.3 Hz, 1H), 7.79 (s, 1H), 7.75 – 7.68 (m, 3H), 7.58 – 7.41 (m, 5H) ppm. $^{13}$C NMR (298 K, 101 MHz, $CDCl_3$) δ: 147.7 (C), 141.1 (C), 137.8 (C), 136.8 (C), 134.9 (1C), 134.8 (1C), 132.3 (CH), 130.6 (2C), 130.5 (C), 130.4 (CH), 128.5 (CH), 128.1 (CH), 127.7 (CH), 127.3 (CH), 127.2 (CH), 126.7 (C), 126.5 (C), 124.4 (CH), 124.3 (CH), 122.5 (CH), 122.3 (2CH), 121.7 (2CH), 118.9 (CH) 118.7 (q, *J* = 320.3 Hz, $CF_3$) ppm.MS (EI), *m/z* (%): 476 (96), 343 (100), 315 (76). HRMS (EI) for $C_{27}H_{15}O_3F_3S$, calculated: 476.0694, found: 476.0712.

**Compound 9**: $^1$H NMR (298 K, 400 MHz, $CDCl_3$) δ: 9.00 – 8.92 (m, 2H), 8.91 – 8.83 (m, 2H), 8.22 (dd, *J* = 7.7, 1.0 Hz, 1H), 8.12 – 8.03 (m, 2H), 7.98 (t, *J* = 7.9 Hz, 1H), 7.84 (dd, *J* = 7.9, 1.0 Hz, 1H), 7.80 – 7.74 (m, 2H), 7.71 – 7.67 (m, 1H), 7.63 – 7.53 (m, 3H) ppm. $^{13}$C NMR (298 K, 101 MHz, $CDCl_3$) δ: 147.9 (C), 134.4 (C), 133.5 (CH), 132.5 (C), 130.8 (C), 130.5 (C), 130.4 (C), 130.2 (C), 129.9 (CH), 129.9 (CH), 129.6 (C), 129.3 (C), 128.6 (CH), 127.8 (2CH), 126.9 (CH), 126.6 (CH), 126.3 (CH), 124.6 (C), 124.5 (CH), 124.4 (C), 124.0 (CH), 123.9 (CH), 122.1 (CH), 121.2 (CH), 120.9 (CH), 118.3 (q, *J* = 320.3 Hz, $CF_3$) ppm. MS (EI), *m/z* (%): 476 (100), 343 (93), 315 (39). HRMS (EI) for $C_{27}H_{15}O_3F_3S$, calculated: 476.0694, found: 476.0701.

3.8. Synthesis of benzo[*l*]indeno[1,2,3-*cd*]pyrene (**P7**)

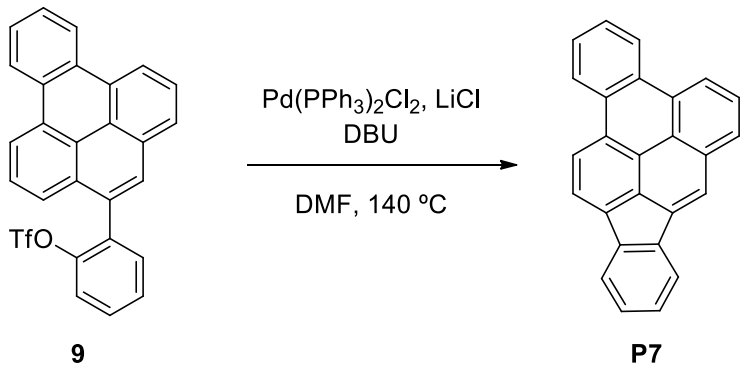


**Figure S12.** Synthesis of compound **P7**.

A sealed tube was charged with triflate **9** (16 mg, 0.034 mmol), $Pd(PPh_3)_2Cl_2$ (7.2 mg, 0.010 mmol) and LiCl (13 mg, 0.31 mmol). The mixture was dissolved in deoxygenated DMF, DBU (18.2 µL, 0.12 mmol) was added and heated at 140 ºC for 16h. The solvent was concentrated under reduced pressure and the residue was purified by column chromatography ($SiO_2$, Hexane/$CH_2Cl_2$ 6:1) to afford compound **P7** (5.5mg, 50%) as a yellow solid. $^1$H NMR (298 K, 750 MHz, $CDCl_3$) δ: 8.94 (d, *J* = 7.7 Hz, 1H), 8.90 (dd, *J* = 7.5, 1.8 Hz, 1H), 8.88 (d, *J* = 7.8 Hz, 1H), 8.85 (dd, *J* = 7.3, 1.8 Hz, 1H), 8.56 (s, 1H), 8.41 (d, *J* = 7.8 Hz, 1H), 8.39 (d, *J* = 7.6 Hz, 1H), 8.14 (d, *J* = 7.2 Hz, 1H), 8.08 (t, *J* = 7.7 Hz, 1H), 8.05 (d, *J* = 7.3 Hz, 1H), 7.81 – 7.74 (m, 2H), 7.50 (td, *J* = 7.3, 1.2 Hz, 1H), 7.46 (td, *J* = 7.3, 1.1 Hz, 1H) ppm. $^{13}$C NMR (298 K, 101 MHz, $CDCl_3$) δ: 141.6 (C), 139.1 (C), 135.6 (C), 134.4 (C), 132.9 (C), 131.2 (C), 130.8 (C), 130.6 (C), 129.4 (C), 129.1 (C), 129.1 (CH), 128.5 (CH), 127.8 (CH), 127.5 (CH), 127.2 (CH), 126.8 (CH), 124.4 (CH), 123.9 (CH), 123.8 (C), 122.6 (CH), 122.0 (CH), 121.9 (CH), 121.7 (CH), 121.5 (C), 121.0 (CH), 120.0 (CH) ppm. MS (EI), *m/z* (%): 326 (100), 163 (27). HRMS (EI) for $C_{26}H_{14}$, calculated: 326.1096, found: 326.1096.

## 4. UV/Vis spectra

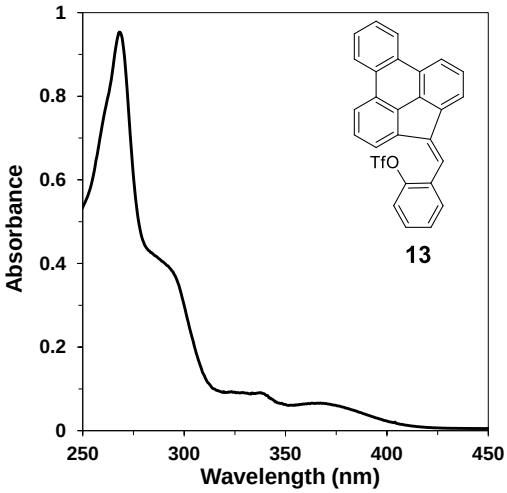


**Figure S13.** Absorption spectrum in $CH_2Cl_2$ of compound **13**

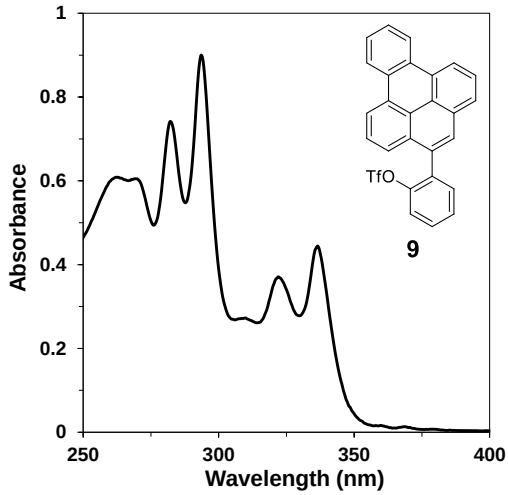


**Figure S14.** Absorption spectrum in $CH_2Cl_2$ of compound **9**

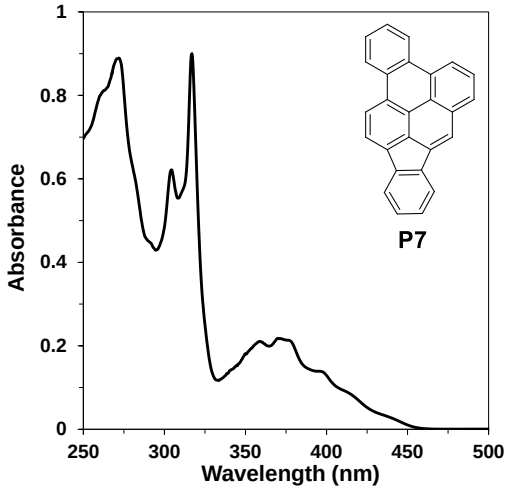


**Figure S15.** Absorption spectrum in $CH_2Cl_2$ of compound **P7**

## 5. $^{1}H$ and $^{13}C$ NMR spectra

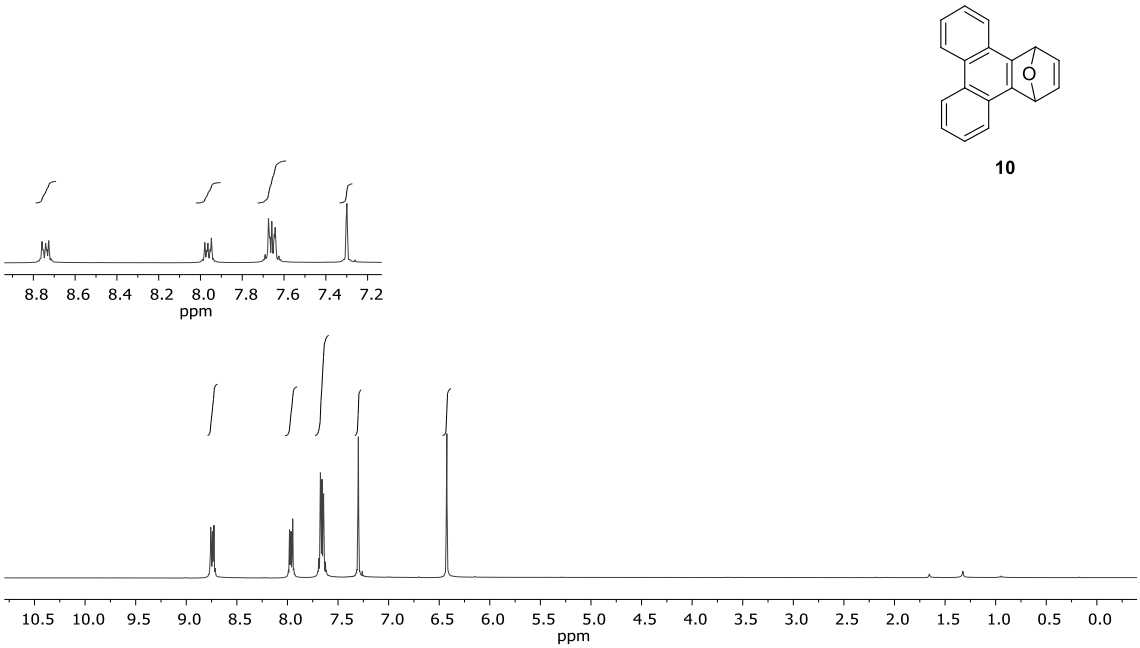


**Figure S16.** $^{1}H$ NMRspectrum of compound **10**.

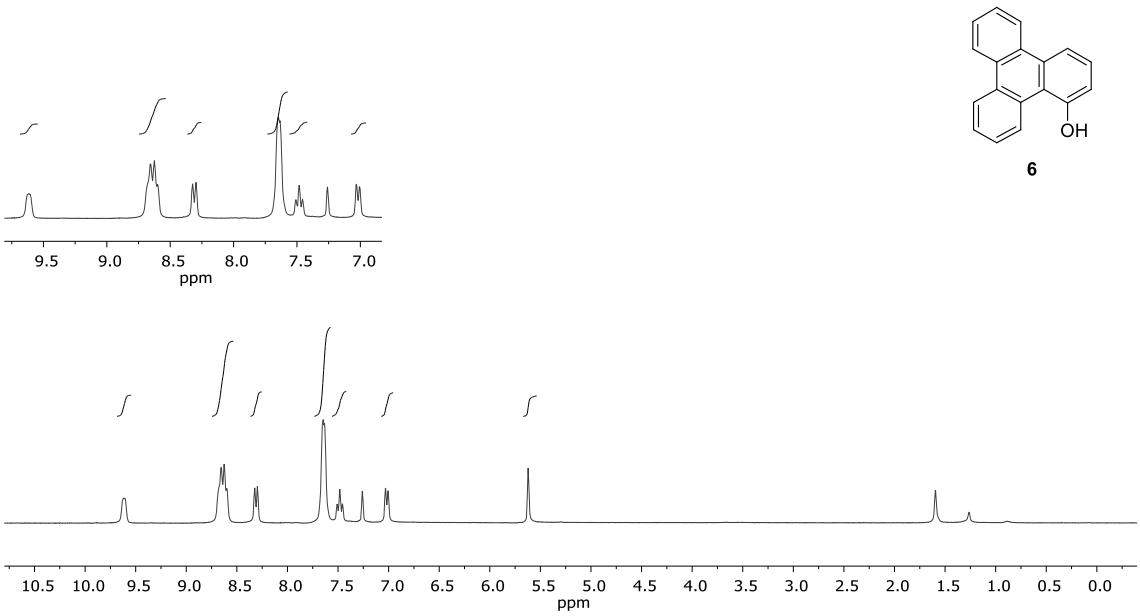


**Figure S17.** $^{1}H$ NMR spectrum of compound **6**.

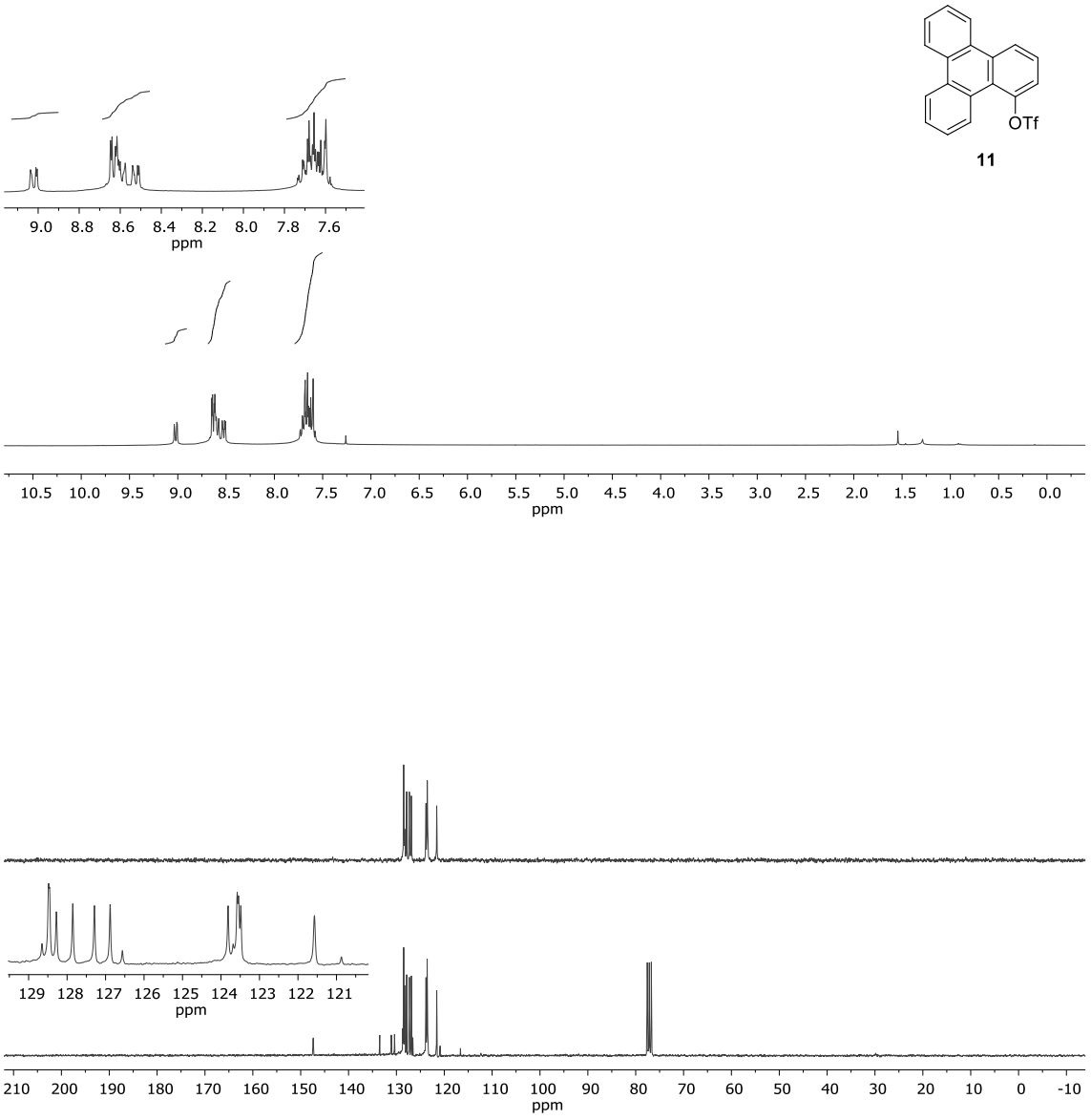


**Figure S18.** $^{1}H$ and $^{13}C$ NMR spectra of compound **11**.

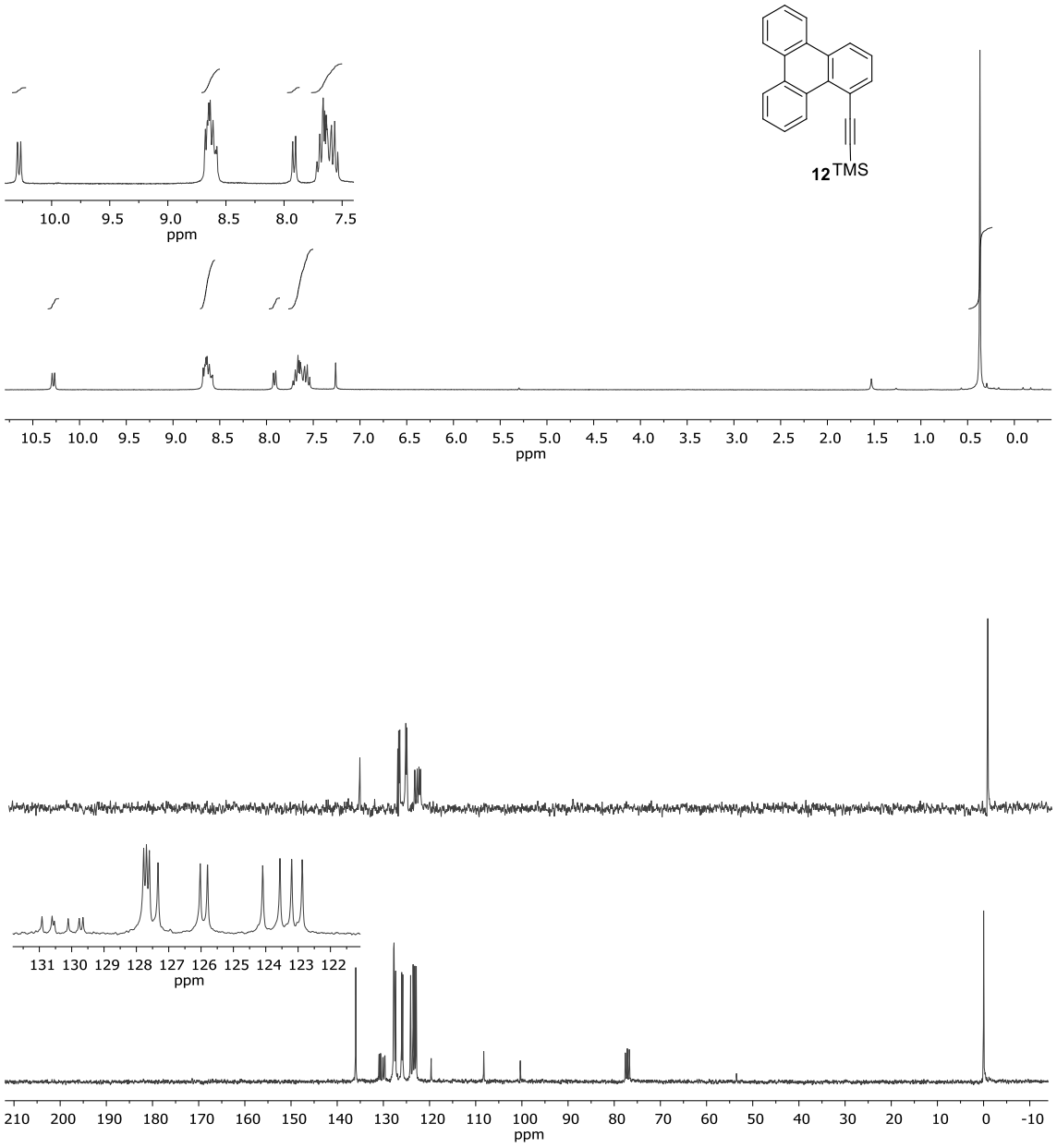


**Figure S19.** $^{1}H$ and $^{13}C$ NMR spectra of compound **12**.

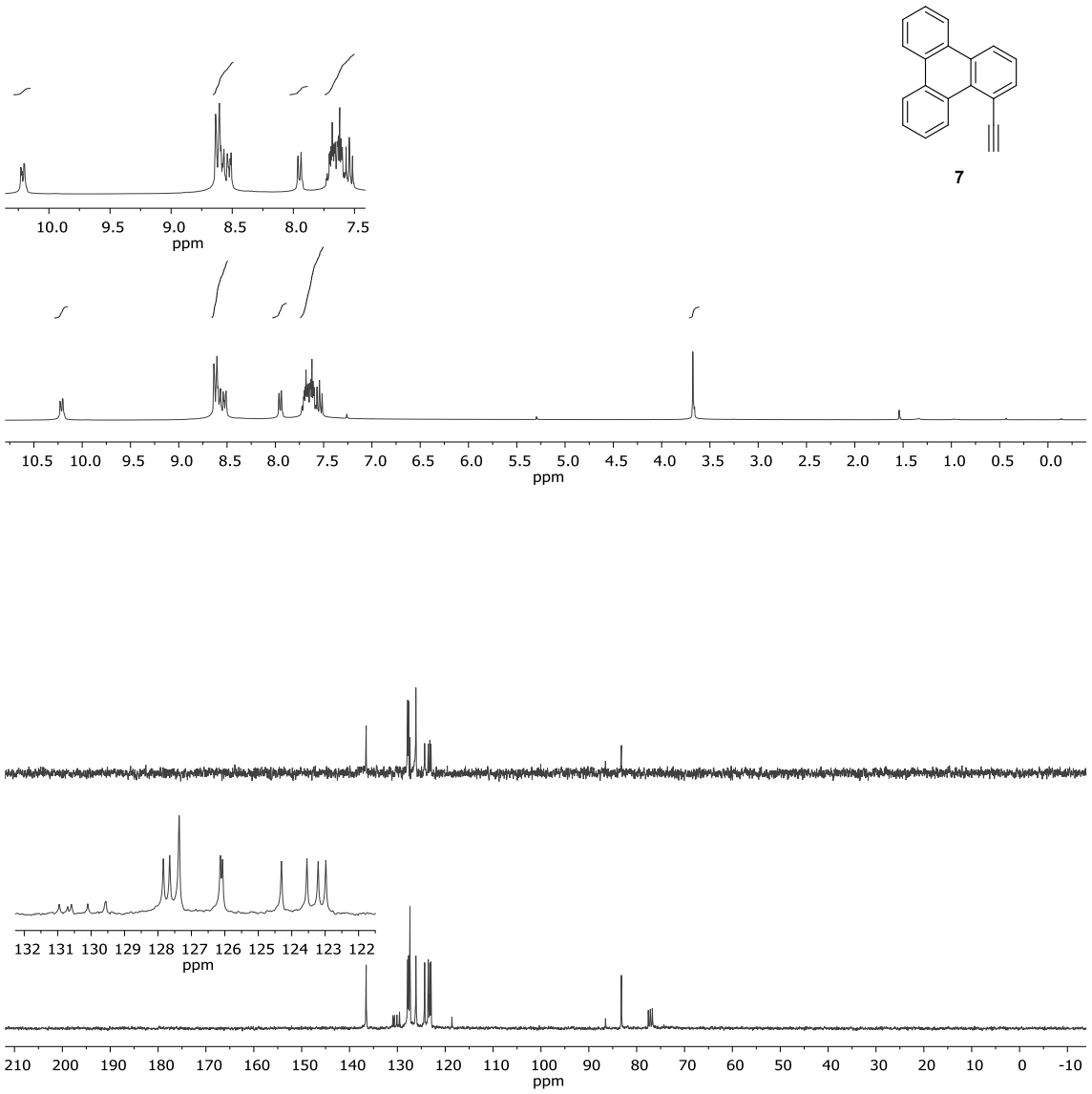


**Figure S20.** $^{1}H$ and $^{13}C$ NMR spectra of compound **7**.

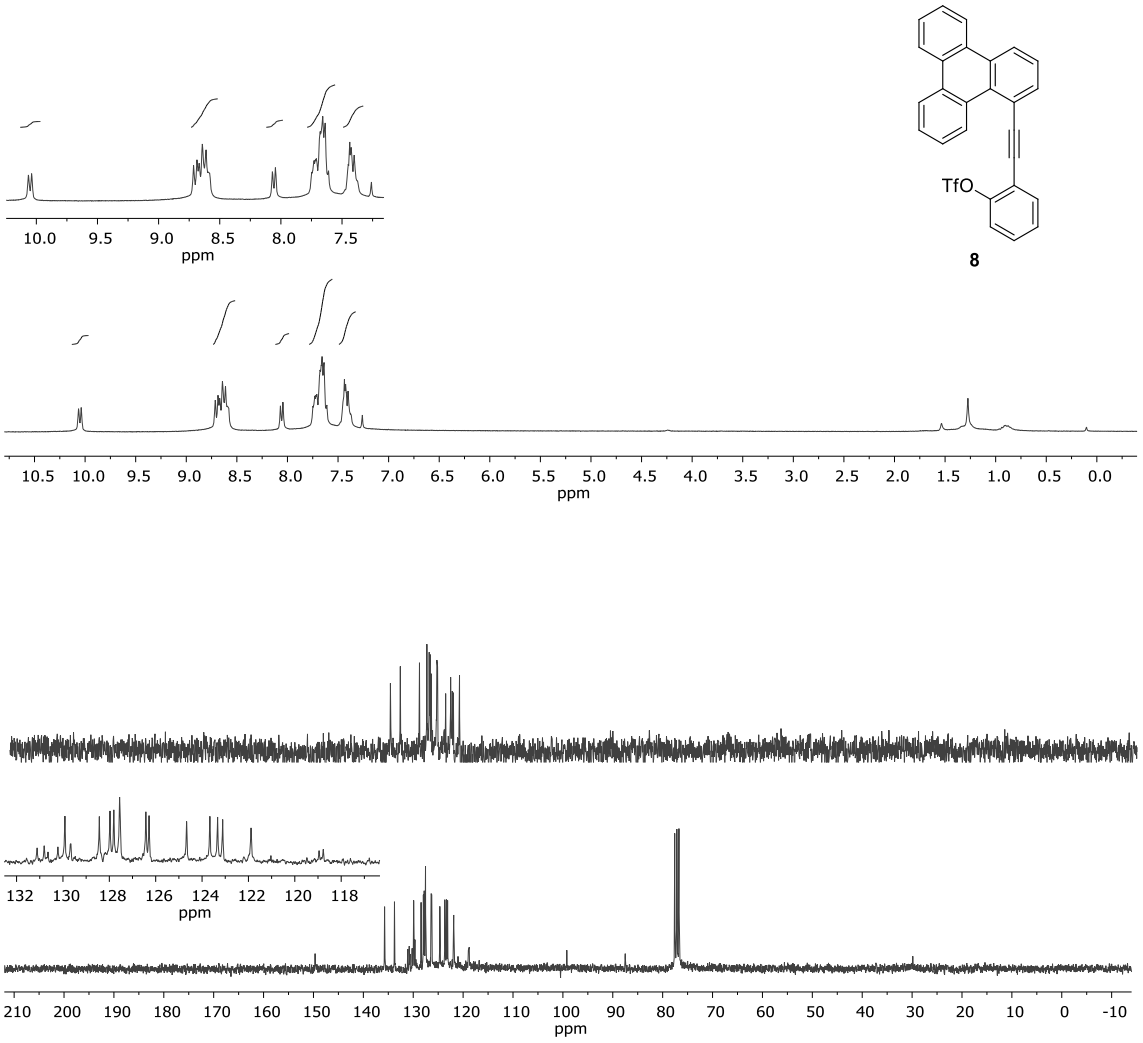


**Figure S21.** $^{1}H$ and $^{13}C$ NMR spectra of compound **8**.

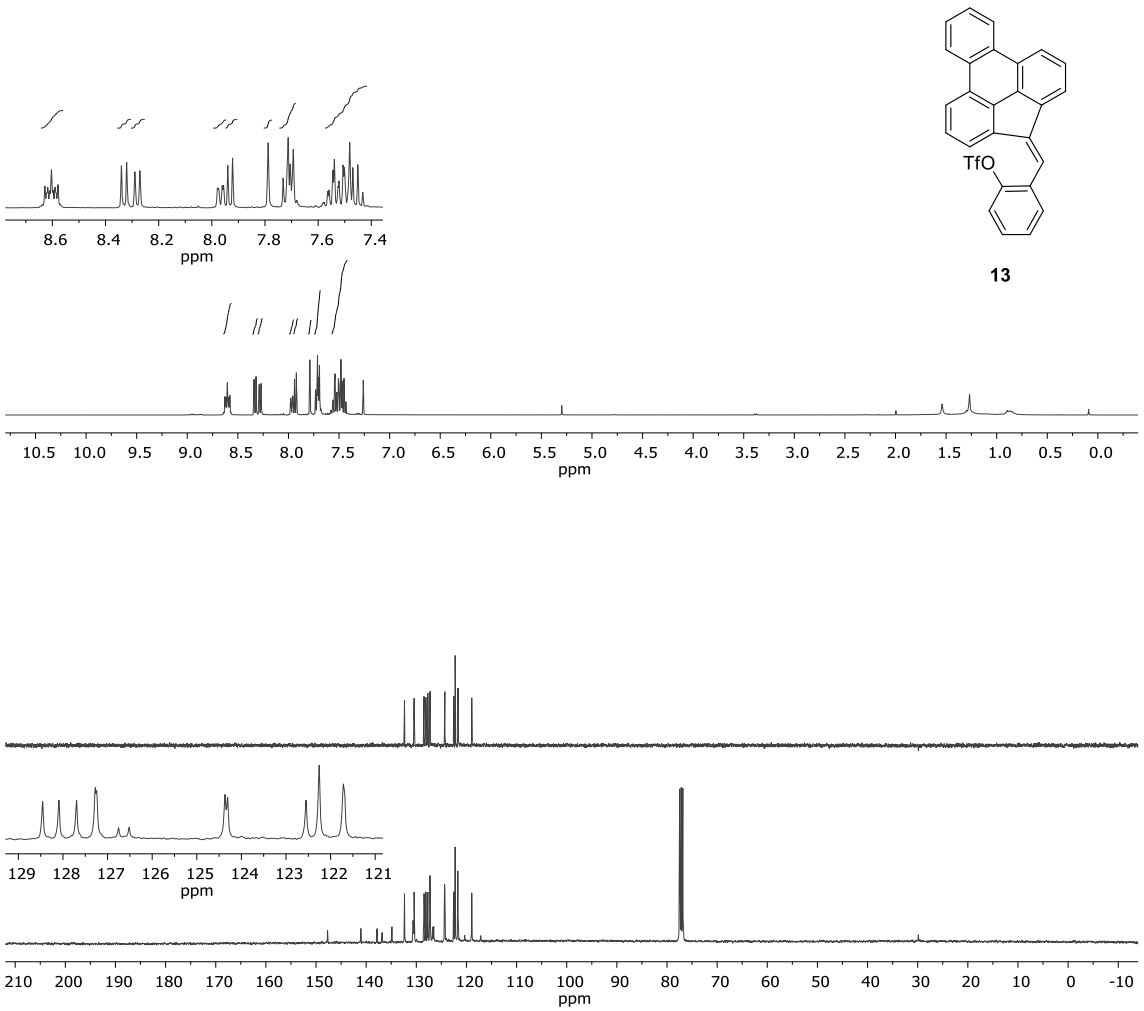


**Figure S22.** $^{1}H$ and $^{13}C$ NMR spectra of compound **13**.

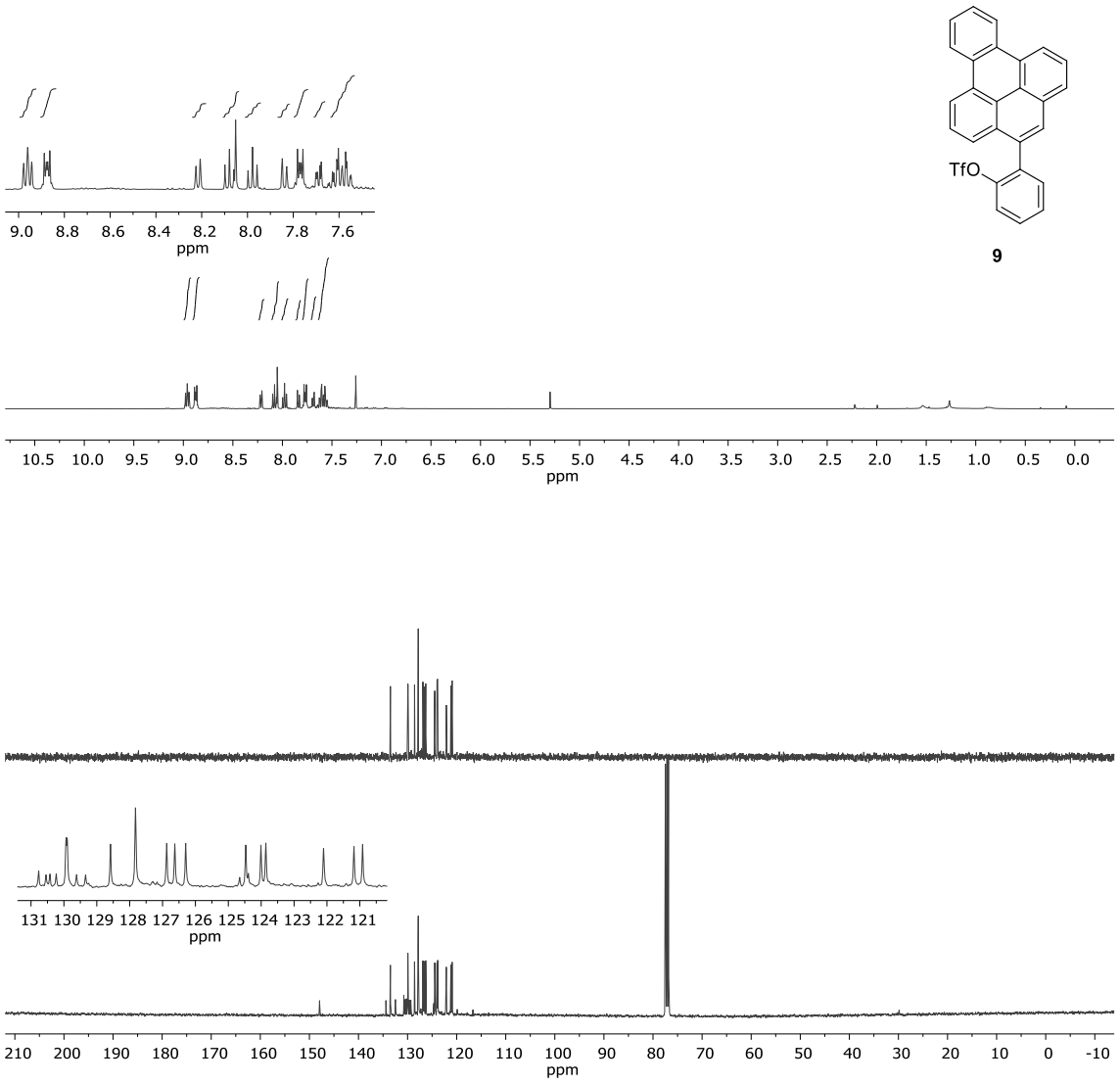


**Figure S23.** $^{1}H$ and $^{13}C$ NMR spectra of compound **9**.

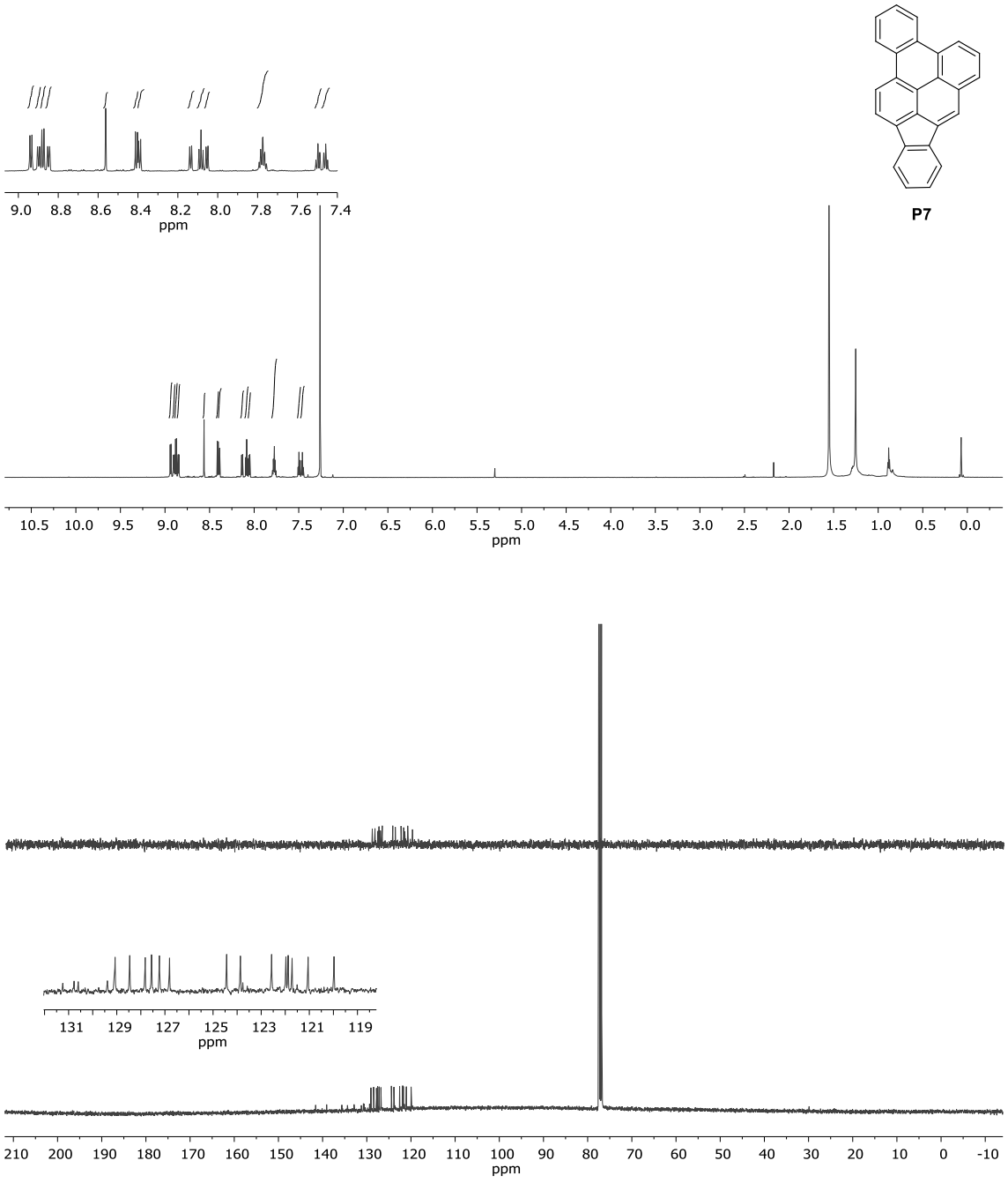


**Figure S24.** $^{1}H$ and $^{13}C$ NMR spectra of compound **P7**.